TECHNICAL REPORT (1): For the Quarter September 1 to November 31, 1988

DARPA ORDER NO: 6560
CONTRACT NO.: N00014-88-C-0684
EFFECTIVE DATE OF CONTRACT: September 1, 1988
EXPIRATION DATE OF CONTRACT: May 31, 1989
PRINCIPAL INVESTIGATOR: L. E. Murr, (503) 690-1026
Department of Materials Science and Engineering
Oregon Graduate Center, Beaverton, Oregon 97006

FUNDAMENTAL AND APPLIED STUDIES OF EXPLOSIVELY FABRICATED HIGH-TEMPERATURE SUPERCONDUCTING FIXTURES

Contributions from: N. G. Eror
C. S. Niou
M. Pradhan
M. Agarwala

CONTENTS

AND INCLUDING 18 FIGURE PLATES (I TO XVIII)

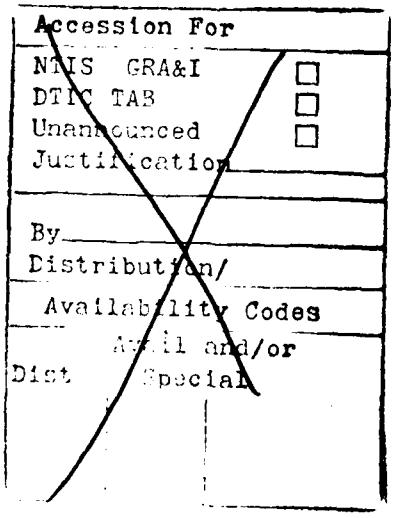

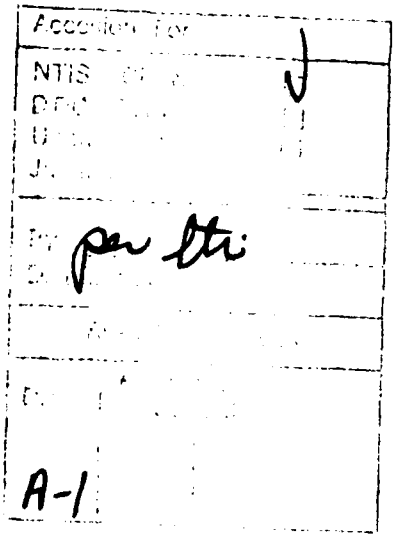

SUMMARY

We have explosively fabricated a wide variety of monolithic superconductor/metal matrix fixtures in a variety of tooling plate geometries, including a design which allowed the channels to be evacuated prior to and during the fabrication process. Tooling plates and fabricated monoliths were utilized in both silver and copper. Channel schedules included pure high-quality $YBa_2Cu_3O_7$ superconducting powder having a size distribution of roughly 0.2 to 20 μm, and mixtures of superconducting (SC) powder with metal powders: 10%, 20%, and 30% silver powder primarily in the silver tooling plate, and the same volume fractions of metal powder loading in copper tooling plates. We were able to demonstrate that tape and ribbon could be easily cold-rolled in a multiple-pass rolling process from explosively-fabricated linear, monolithic precursors by as much as 95% (to a tape thickness of 0.15 mm). The silver tapes have the convenience of allowing for an annealing treatment or treatment series which can connect the superconducting tape core for supercurrent transport.

We have utilized and are further developing a more fundamental understanding for qualitative evidence for superconducting powder starting quality and its alterations or degradation following explosive fabrication. In this diagnostic approach, we examine the $2\Theta = 32°$ and 58° orthorhombic split-peak x-ray profiles which appear to be extremely sensitive to non-superconducting fractions and non-stoichiometric or oxygen-disordered regions. These peaks, when resolved, appear to represent signatures for the high-Tc superconducting phase, and small changes can be readily observed in the qualitative (and quantitative) changes of these split-peak signatures. Using this simple observational approach, we have examined the superconducting powders placed in the tooling plate channels prior to explosive fabrication and after fabrication to provide some diagnostic evidence of whether the fabrications or the fabrication parameters were being optimized, or whether the experimental direction we were taking was one toward optimization. We observed, in fact, in a series of experiments that these x-ray split peak signatures were measurably degraded, leading us to the conclusion that our methodology was going in the wrong direction. These observations will allow us to re-examine the fabrication process and make necessary design and parametric changes.

We have begun to look at the effect of metal loading on the residual superconducting behavior of fabricated monolithic mixtures. These mixtures exhibit a prominent Meissner effect and levitation of a magnet, and we will quantify the effect of volumetric loading on these effects. This approach may provide some means of calibrating the superconducting and non-superconducting fractions in the starting powder which have been of great concern in this process since the most significant feature of explosive fabrication is the production of a conformal, metal-matrix-supported monolith which has an intrinsic superconducting application; and will require little, if any, additional processing or treatment.

We have demonstrated the ability to scale the explosive fabrication process, and we have not observed significant effects of superconducting channel geometries/cross sections on the fabrication quality. However, we have not achieved consolidation within the channels in excess of 90%

density, and we have not determined whether or not evacuation is essential in the process steps or the tooling array sizes we have utilized thus far.

INTRODUCTION

We have demonstrated in preliminary work that explosive (shock-wave) fabrication appears to pose an attractive prospect for producing simple, conformal superconducting fixtures utilizing the new high-temperature copper-oxide-based ceramic powders (1-3). We have demonstrated the feasibility of placing $YBa_2Cu_3O_7$ superconducting powder within a metal matrix, such as copper, to create a monolithic structure which encapsulates and protects the reactive superconductor, and imposes its own strength and "workability" on the brittle and mechanically uncooperative superconductor. Furthermore, since passage of a strong shock wave through a crystalline material creates residual defects in its structure, it was originally thought that such defects would further enhance the utility of this fabrication concept by rendering the ceramic superconductor slightly ductile by creating large densities of dislocations, and/or improving the superconducting behavior by creating other defects which would trap flux and increase the current density or possibly elevate the critical temperature, critical field, or all of these critical parameters (1-3).

While we have, in fact, observed that monolithic structures can be fabricated explosively (1-3), superconductivity, as measured by residual diamagnetic and resistive behavior, is erratic. That is, while many samples exhibited large Meissner effects (as evidenced by levitation of magnets above explosively fabricated fixtures), supercurrent (d.c.) transport was erratic at best. Current densities in simple linear fixtures were observed to be as high as 4×10^3 Acm^{-2} in direct transport experiments where currents in excess of 500 amperes were passed through a two-terminal bus at zero voltage (3). But after a few cycles, the transport ceased. Furthermore, the density of microtwins in $YBa_2Cu_3O_7$ increased by 10 to 20

times after explosive fabrication, but quantitative measurements of any effect on current density have not been possible, although qualitative inferences about flux pinning were discussed (3).

One of the important aspects of this fabrication process--explosively fabricating superconducting metal-matrix composites--is the ability to produce an applicable superconducting fixture with an immediate application which does not require additional processing or manufacturing to work. This means that the explosive process must consolidate the superconducting powder and bond it to the supporting metal or alloy matrix to create electrical connectivity able to transport supercurrent. To do this, the high-pressure process must be "optimized" to keep heating to a minimum to avoid surface melting or reactions at superconducting particle surfaces which would cause microstructural or chemical degradation producing non-superconducting phase regimes while producing a dense consolidation of the powder. This requires some requisite peak pressure and some attention to particle size and, more importantly, size distribution as well as some concern for trapped gases causing adiabatic heating (4).

We used our best guesses and judgemental experience in executing several preliminary fabrications of $YBa_2Cu_3O_7$ powder in both copper and aluminum matrices, but it was clear that a more fundamental series of experiments was required to begin to produce more dependable and more optimized fixtures. This research program represents a first attempt at a more systematic understanding of optimum fabrication parameters.

EXPERIMENTAL CONSIDERATIONS AND OBJECTIVES

Since this fabrication process attempts to produce superconducting fixtures which do not require heat treatment or extensive re-fabrication or

manufacturing, the initial quality of the starting superconducting powder is a crucial feature of the experimental program. Plate I illustrates this phenomenon. Several issues are depicted schematically in Plate I. These include: (1) the prospects of having powders which include a non-superconducting phase or a phase which has a much lower T_c, thereby reducing the overall T_c by a rule of mixtures, and (2) the prospects for high-quality, single-phase powder to become rapidly reacted at their surfaces, forming a non-superconducting phase which, when explosively consolidated, would create an interfacial phase much larger than the average coherence length, and leading to a "disconnected" regime insofar as supercurrent transport is concerned. We have, in fact, examined some of these issues in preliminary research (5).

In our work, it is also necessary to prepare significant quantities of high-quality powder because the tooling plates we use contain an array of conformal machined (milled) channel geometries into which superconducting powder is placed. These tooling plates (base plate in the illustration in Plate II) usually require several hundred grams of powder at a minimum.

The determination of the superconducting fraction in a powdered sample is difficult to define rigorously. For example, from first principles we can write:

$$\underset{\sim}{B} = \underset{\sim}{H} + 4\pi\underset{\sim}{M} \qquad (1)$$

where $\underset{\sim}{M}$ is the intensity of magnetization defined as the vector sum <u>per unit volume</u> of the magnetic moments of the Amperian current loops. An alternative scalar form can be written (in emu):

$$B = H\,(1 + 4\pi\chi) \qquad (2)$$

For a diamagnetic material (a superconductor), the current in the equivalent loop is zero when there is no applied field. This means, of course, that there is no resistance in these equivalent current loops. It also means that the sign of χ (the magnetic susceptibility) will be negative. Clem (6) among others, has examined the "granular" features of ceramic superconductors depicted schematically in Plate I and writes:

$$(1 + 4\pi\chi) = f_n + f_{sc}\,[1 - P_{cyl}\,(R_g/\lambda_g)] \qquad (3)$$

where $(1 + 4\pi\chi)$ (sign of χ being negative) is the effective temperature-dependent permeability of the granular material, f_n and f_{sc} are the normal or non-superconducting and superconducting fractions, respectively, (unshaded and shaded regions in Plate I) for a single cylindrical grain having a radius R_g, and λ_g is the depth to which a small magnetic field applied to the sample will penetrate the cylindrical grain. P_{cyl} in Eqn. (3) is a factor by which magnetic flux penetration suppresses a cylindrical grain's magnetization below that expected for complete Meissner-state flux exclusion (7).

Equation (3) represents a single, idealized grain which is modelled ideally by the extreme upper left illustration in Plate I. To extend this to an aggregate of grains in a sample would require redefining P_{cyl} and R_g in terms of the sample geometry and size. There is a temperature dependence of λ_g and it will also be influenced by microstructural partitioning (or repartitioning) of the grain, etc. In the most general case, we can rewrite Eqn. (3) as:

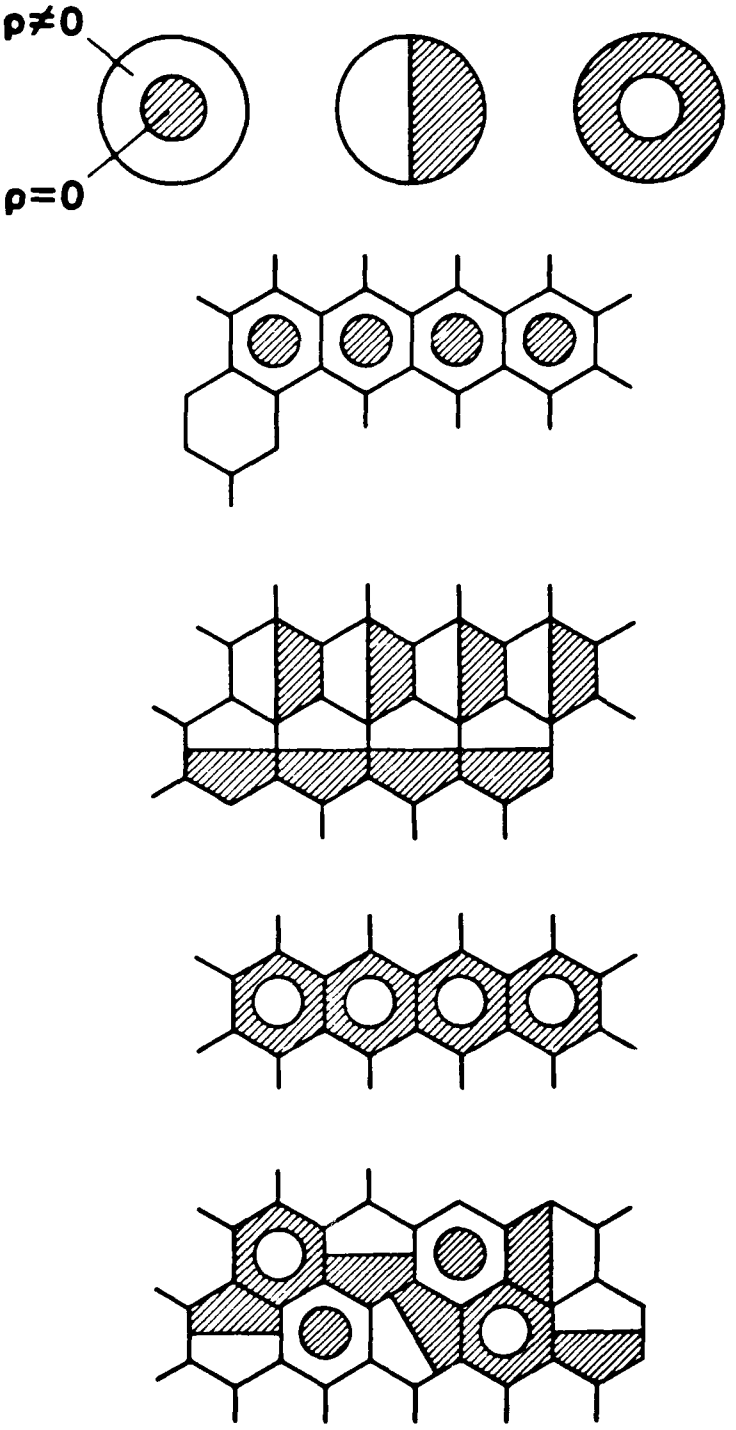

Plate I

$$(1 + 4\pi\chi) = f_n + \xi f_{sc} \tag{4}$$

where ξ is a rather complex geometrical factor which will change with the distribution of the grain size, the geometry of the grains (or superconducting powder particles), the geometry of the sample actually measured, etc. We might even assume that $f_n + f_{sc} = 1$ and rewrite:

$$(-4\pi\chi) = f_{sc}\,(\xi-1) \tag{5}$$

In other words, measuring susceptibility as $(-4\pi\chi)$ will never yield absolute values nor possibly even sensible values for f_s (the superconducting fraction) unless the geometrical coefficient in Eqn. (5) can somehow be determined:

$$(-4\pi\chi) = \xi' f_{sc} \tag{6}$$

This might be done experimentally by performing susceptibility measurements on a fixed sample volume and geometry having a constant density and a constant particle size and shape (or distribution of particles having a constant shape). The factor, ξ', in Eqn. (6) will also be sensitive to the location of the non-superconducting fraction, that is to the distribution or displacement of the superconducting and non-superconducting fractions in individual particles as shown in Plate I. The likelihood of developing an accurate calibration for ξ' in Eqn. (6) seemed remote at best since measurements of magnetic susceptibility, in fact, were observed to vary by factors of two or more for measurements on the same samples by different laboratories.

Furthermore, we were concerned about developing a simple diagnostic tool which would allow us not only to assess the quality of our starting superconducting powder ($YBa_2Cu_3O_7$), but to compare this assessment with the consolidated superconductor in an explosively fabricated fixture (Plate II). The magnetic susceptibility measurement in Eqn. (6) would be further compromised by the microstructural changes created by the attendant shock wave.

We looked to x-ray diffraction as a very simple and possibly reliable qualitative diagnostic tool. However, since x-ray diffraction has been discounted as too macroscopic and insensitive, we examined the spectrum for potentially reliable guidelines in the orthorhombic $YBa_2Cu_3O_7$ powder. What we found was a very interesting and very characteristic evolution of peak splitting around $2\theta = 32°$ and $2\theta = 58°$ as illustrated in Plate III. We have described these features in detail (8), but for continuity here we should point out that [1] to [4] show the evolution of the superconducting, orthorhombic structure during solid-state (high-temperature) reaction. The intriguing feature is the tetragonal precursor at [2] which begins to split at [3] just prior to the evolution of the stable $YBa_2Cu_3O_7$. We believed this evolution could, along with the "shaper" of the split peaks at [4], provide at least a qualitative perspective.

To test this approach, we compared the split-peak "signatures" at $2\theta = 32°$ and 58° for our "best" powders prepared by solid-state reaction and freeze drying with some of the "best" available commercial powder. In making this comparison, shown in Plate IV, we also attempted to quantify the split-peak "signatures" by taking the ratio of peak areas, and these are shown in Plate IV. (a) shows two solid-state reacted powders [SS] and [SSX] and two freeze-dried powders [FD(1)] and [FD(2)], while (b) shows two

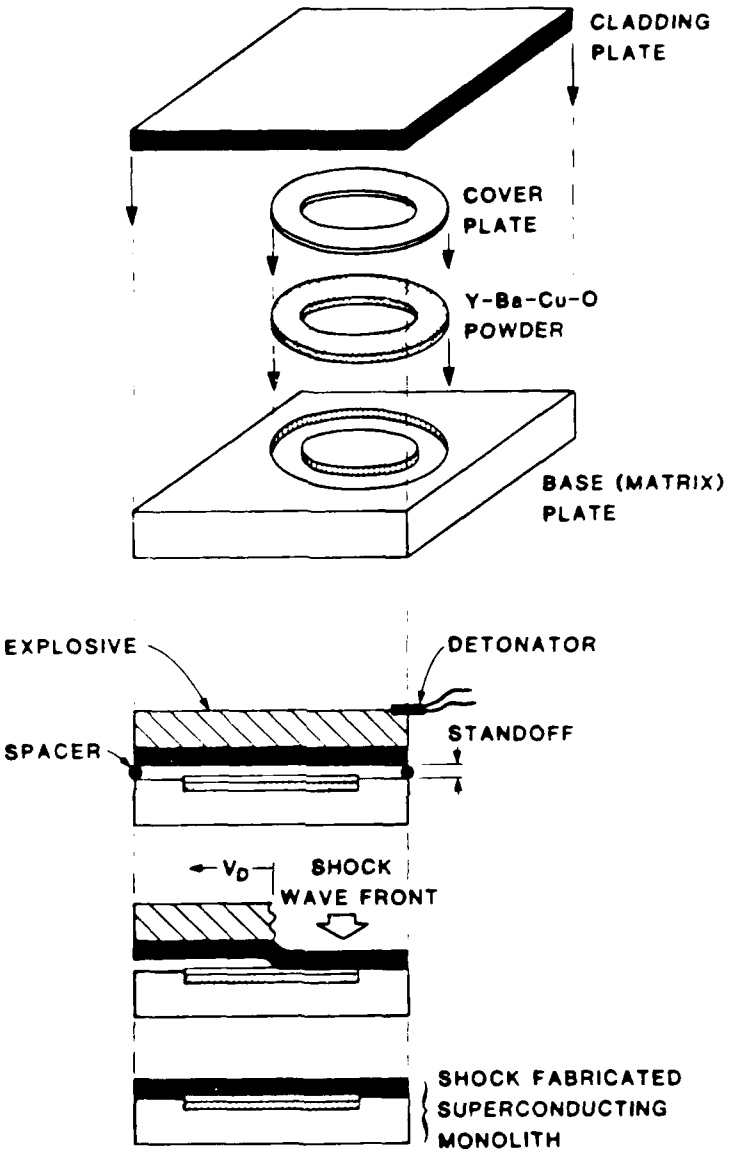
CLADDING
PLATE
COVER
PLATE
Y-Ba-Cu-O
POWDER
BASE (MATRIX)
PLATE
EXPLOSIVE
DETONATOR
SPACER
STANDOFF
V_D
SHOCK
WAVE FRONT
SHOCK FABRICATED
SUPERCONDUCTING
MONOLITH

Plate II

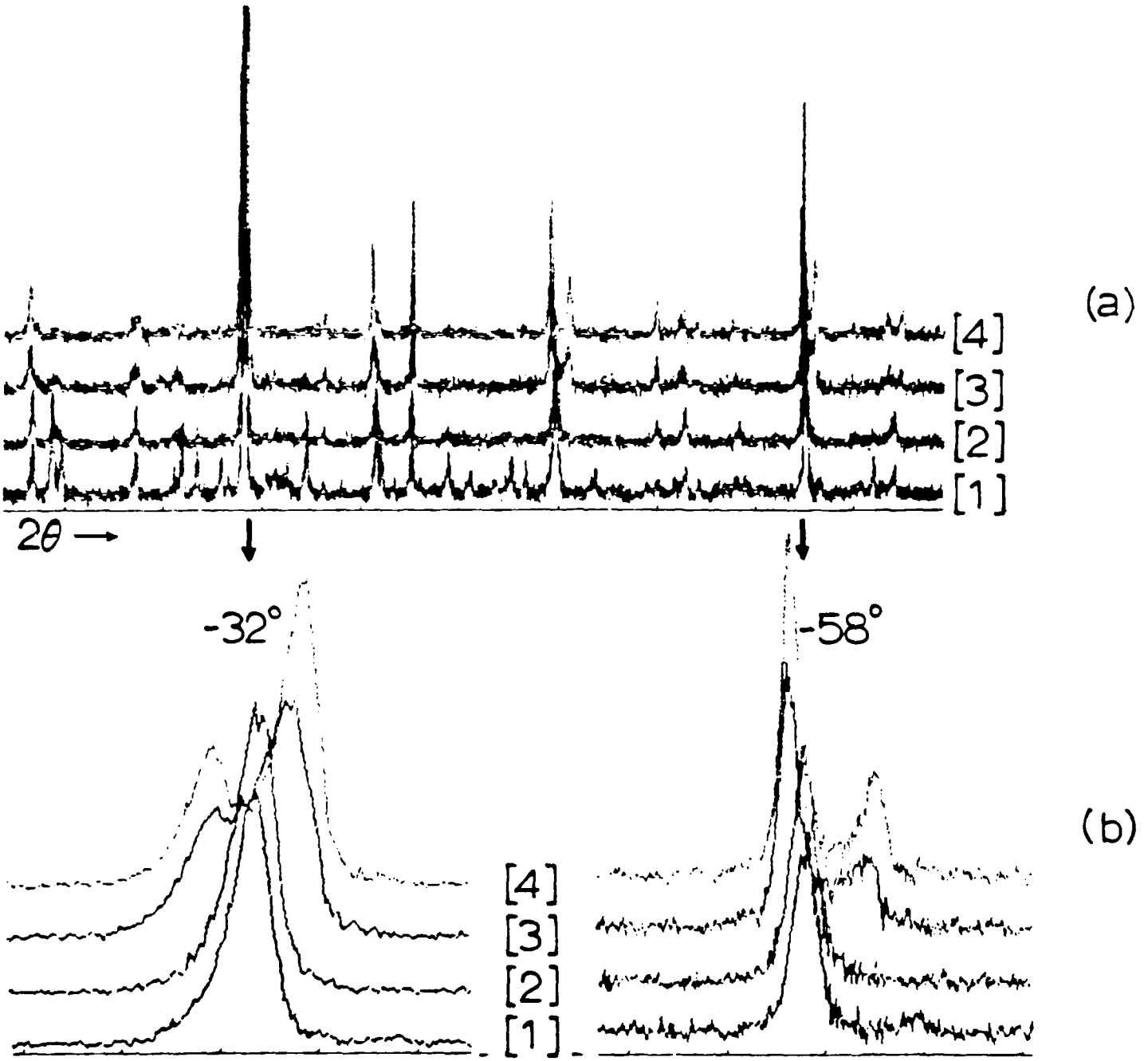

Plate III

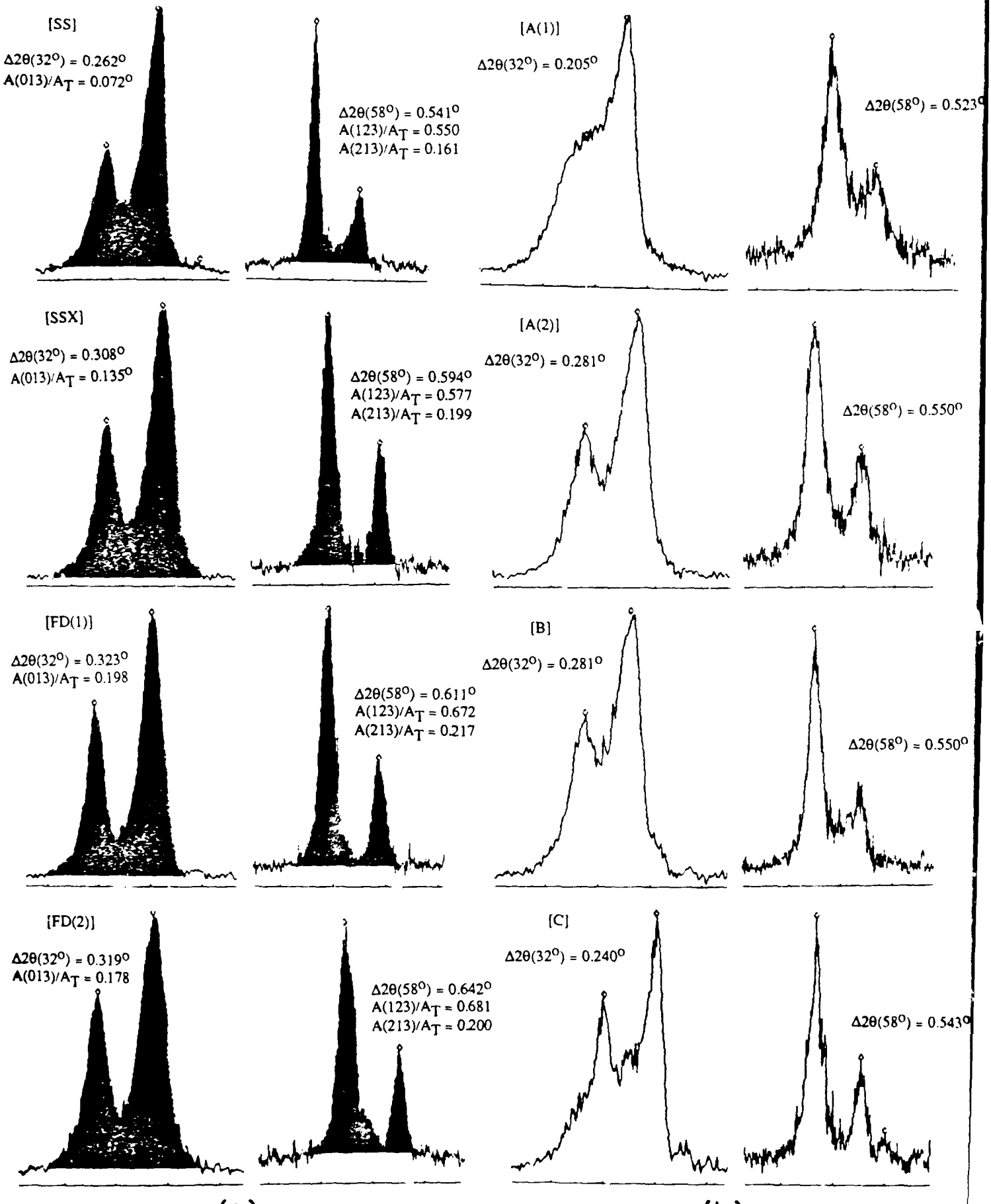
[SS]
Δ2θ(32°) = 0.262°
A(013)/A_T = 0.072°
Δ2θ(58°) = 0.541°
A(123)/A_T = 0.550
A(213)/A_T = 0.161
[A(1)]
Δ2θ(32°) = 0.205°
Δ2θ(58°) = 0.523°
[SSX]
Δ2θ(32°) = 0.308°
A(013)/A_T = 0.135°
Δ2θ(58°) = 0.594°
A(123)/A_T = 0.577
A(213)/A_T = 0.199
[A(2)]
Δ2θ(32°) = 0.281°
Δ2θ(58°) = 0.550°
[FD(1)]
Δ2θ(32°) = 0.323°
A(013)/A_T = 0.198
Δ2θ(58°) = 0.611°
A(123)/A_T = 0.672
A(213)/A_T = 0.217
[B]
Δ2θ(32°) = 0.281°
Δ2θ(58°) = 0.550°
[FD(2)]
Δ2θ(32°) = 0.319°
A(013)/A_T = 0.178
Δ2θ(58°) = 0.642°
A(123)/A_T = 0.681
A(213)/A_T = 0.200
[C]
Δ2θ(32°) = 0.240°
Δ2θ(58°) = 0.543°
(a)
(b)

Plate IV

different lots of vendor A powders [A(1) and A(2)] and vendor B and C powders. We also looked at shifts in the peak centroids ($\Delta 2\Theta$) as a quantitative feature. Without a great deal of discussion, it is readily apparent that there is a marked difference between the x-ray split-peak signatures. We also attempted to "quantify" the superconducting powders on the basis of the Meissner strength or, more simply, the levitation height of a standard magnet over a standard volume of pressed pellet.

While x-ray peak splitting cannot distinguish the location of non-superconducting material or provide any detailed spatial information, it did provide some assurance that our starting powders had a reasonably high superconducting fraction (possibly 90%), and the signatures might provide some reasonably accurate, qualitative guidelines. That is, degradation of the superconducting powder could be observed in alterations in the split-peak "shapes" (or signature). But the distribution of f_n (Eqn. 4) is unknown.

We were also concerned initially with the actual crystallite size and the particle size distribution in the superconducting powders because the particle size distribution has an important influence on the consolidation efficiency and the actual (high-pressure state) and residual temperatures as well as the distribution of thermal "hot spots" (4).

The initial or near-term objectives of this research program involved an effort to develop a schedule of optimum parameters for the efficient fabrication of monolithic superconductors (Plate II) in the high-pressure state. One of the most obvious parameters was initially considered to be the peak pressure, which, in the experimental arrangement shown in Plate II, is related to the detonation velocity of the explosive.

Our preliminary work established what we assumed to be a fabrication window bounded by pressures ranging from about 3 to 30 GPa in the superconducting channels (Plate II). The upper limit of pressure was determined from a cylindrical (or axisymmetric) geometry (5); and by modifying this geometry using an explosive consolidation fixture developed at Los Alamos National Laboratory (4), we hoped to narrow the pressure required to optimize powder consolidation in the planar geometries illustrated in Plate II. Unfortunately, the accompanying pressure hydrocode for the Los Alamos fixture required extensive reworking for detonation velocities below about 4500 m/s. We have chosen to concentrate on low-detonation velocity processing using ANFO (Ammonium Nitrate and Fuel Oil mixtures) where detonation velocities (V_D) can be varied from about 1800 to 3200 m/s.

With a late start in our experimental program and in the absence of more fundamental pressure versus consolidated density data, we designed our first tooling plates to accommodate a wide range of experimental features. These included powder mixtures--mixtures of metal powders such as copper and silver--with $YBa_2Cu_3O_7$ powder. We were also interested in examining the prospects for heat treatment of channels which might be degraded by incorrect process parameters (poor fabrication) and the use of explosively fabricated precursors for tape or ribbon production and the potential for or necessity for heat treating the ribbon or tape to produce a "connected" superconducting core capable of passing d.c. supercurrent.

We were also initially concerned about the effects of trapped gas within the channels although we did not see any significant effects during our preliminary research (1-3). In addition, we speculated that degradation of the superconducting $YBa_2Cu_3O_7$ powder might occur by oxygen loss in the high pressure state and thought that a mixture of AgO could help to

stabilize the oxygen or provide a mechanism to reoxygenate the channels by heat treatment after explosive fabrication. To heat treat fixtures required a non-reactive matrix such as silver. We, therefore, designed both silver and copper tooling plates as shown in Plate V.

The channel geometries and configurations shown in Plate V were designed to begin to illustrate possible effects of the jetting (collision velocity) direction and the effects of channel cross sections or aspect ratios. The channel geometries were also arranged for convenient extraction without exposing other fixtures. Simple cylindrical buttons were placed in the tooling plates (0.5 inches thick) to act as quick reference locations to test the residual Meissner effect and provide x-ray diagnosis prior to examining the linear channels.

The detonation velocity used in fabricating the Ag and Cu tooling plates (Plate V) was 2200 m/s, adjusted upward from our preliminary work to attempt better powder consolidation. The cladding plate was 1/8 in. copper or silver and an equivalent standoff distance was used with approximately 4 inches of explosive (ANFO mix). (1 inch = 2.54 cm).

Summary of the Initial Program Objectives

1. Production and characterization of several kilogram batches of good quality $YBa_2Cu_3O_7$ powder having a distribution of particle sizes (we routinely produced a distribution of < 0.2 μm to 20 μm).

2. Design and explosive fabrication of several experimental assemblies containing various conformal geometries to optimize channel geometries and to optimize the fabrication pressure and other critical parameters--even the identification of what the critical parameters are for the fabrication geometry shown in Plate II (see Plate V).

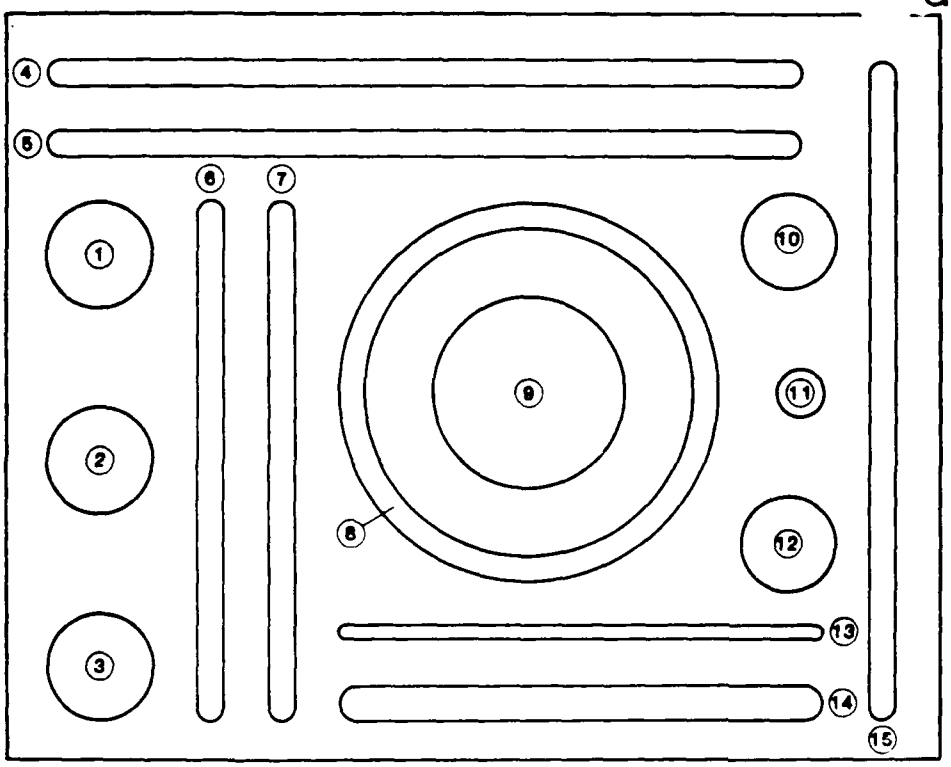

(8"x10")

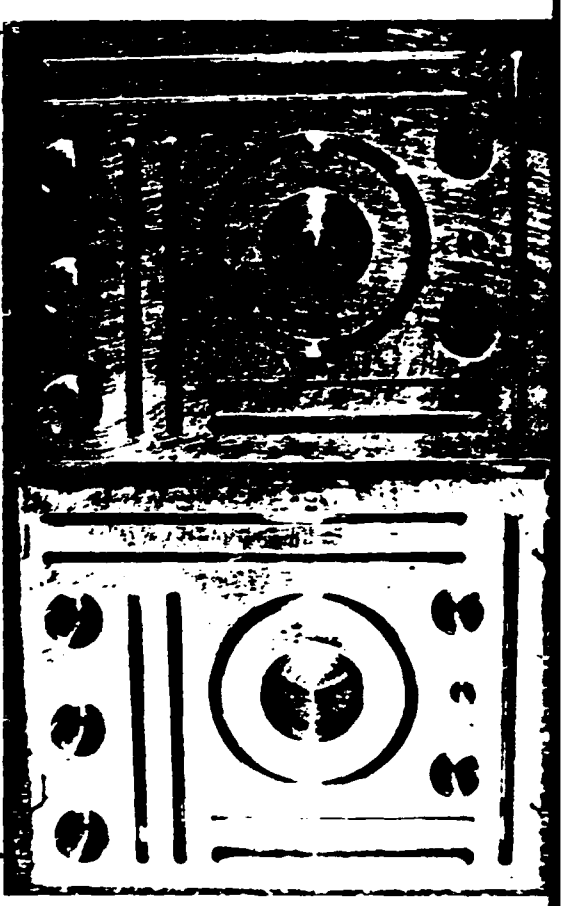

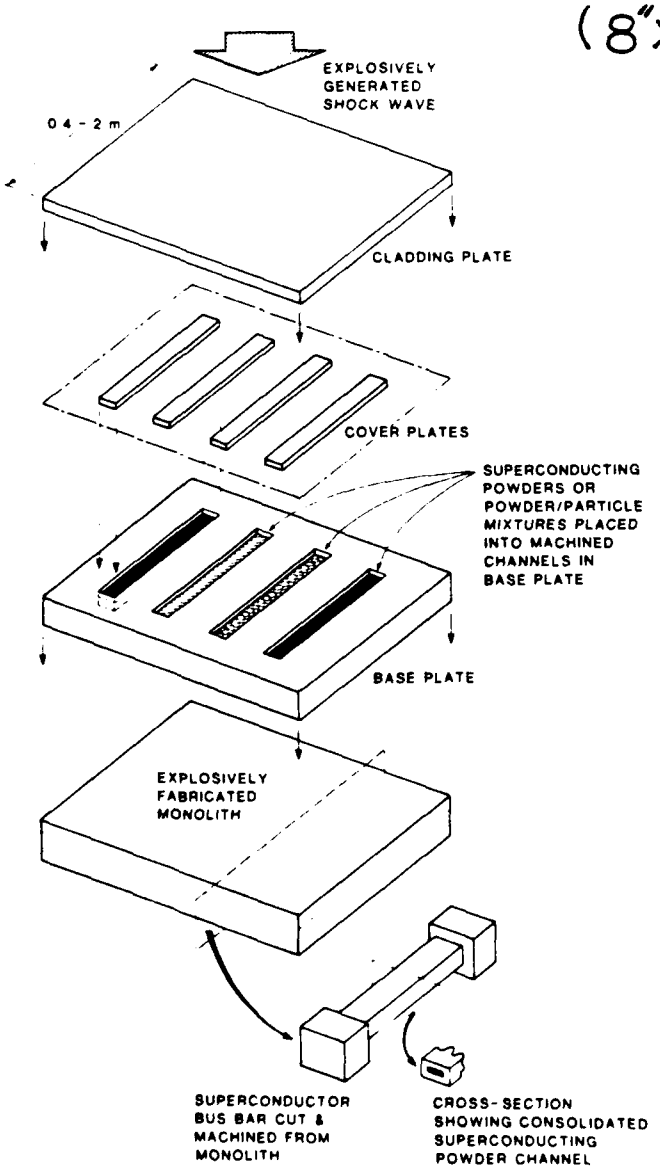

CHANNEL LOADING SCHEDULE		
CHANNEL #	Ag TOOLING PLATE	Cu TOOLING PLATE
1	SC* + 10% Ag Powder	SC + 10% Cu Powder
2	100% SC	100% SC
3	SC + 30% Ag Powder	SC + 30% Cu Powder
4	SC + 10% Ag Powder	SC + 10% Cu Powder
5	SC + 30% Ag Powder	SC + 30% Cu Powder
6	SC + 20% Ag Powder	SC + 20% Cu Powder
7	100% SC	SC + 10% Ag Powder
8	100% SC	100% SC
9	100% SC	100% SC
10	100% SC	100% SC
11	100% SC	100% SC
12	SC + 10% AgO Powder	SC + 30% Ag Powder
13	100% SC	100% SC
14	SC + 10% AgO Powder	SC + 30% Ag Powder
15	SC + 30% Ag Flake	100% SC

*SC = Superconductor ($YBa_2Cu_3O_7$) Powder

Plate V

3. The design of silver and copper tooling arrays to allow for heat treatment of explosively fabricated fixtures and to heat treat ribbon or tape processed from monolithic precursors (Plate V).

4. This program, in conjunction with Monolithic Superconductors, Inc. and in cooperation with Los Alamos National Laboratory sought to utilize the laboratory's hydrocode to optimize pressure for fabrication of superconducting monoliths and to measure magnetic susceptibility as well as other superconducting properties where appropriate. Provision of Los Alamos with precursor examples for tape/ribbon processing (Plate V).

5. Characterization, using optical metallography, x-ray diffraction, SEM, etc., of the experimentally fabricated fixtures to be fabricated, as illustrated in Plate V.

6. Examination and assessment of commercial potential and market development for simple, conformal superconducting geometries in monolithic fixtures illustrated typically in Plate V; in conjunction with Monolithic Superconductors, Inc.

7. Critical assessment of fabricated fixtures, fabrication parameters, and superconducting powders and properties before and after explosive fabrication to determine design changes, etc. in order to converge on the process optimization alluded to in 2) above.

RESULTS AND DISCUSSION OF Ag AND Cu TOOLING PLATE FABRICATIONS (PLATE V)

Plate VI illustrates some examples of the starting superconducting (SC) powder, numerous fixtures extracted from the Ag and Cu explosively fabricated tooling plates (including the powder mixtures--Plate VI shows an example of a SC + 10% Ag channel mixture in the Ag tooling plate), and the prominent Meissner effect observed for test buttons--showing a 4 mm magnet levitating over a SC + 10% Cu mixture in a copper matrix. While essentially all fabricated channels (Plate V) exhibited residual diamagnetism (as evidenced by levitating magnets as in Plate VI), and most linear channels were electrically continuous, no superconducting transition was observed, and the resistivity increased with decreasing temperature to 77 K, indicative of semiconductor behavior.

We examined selected channels in both the Cu and Ag tooling plates after explosive fabrication using the split-peak x-ray diagnostics. Selected results are illustrated in Plates VII and VIII. The x-ray split-peak "signatures" are observed to be altered and slightly "degraded". We are not sure what the alteration means, but we are investigating these features in great detail--including attempts to isolate the tetragonal precursor shown at [2] in Plate III. We are particularly interested in this precursor because it could explain in part the split-peak adjustments observed. It seems unlikely that a significant oxygen loss is involved because the low-oxygen tetragonal structure ($YBa_2Cu_3O_6$ ideal structure) would be significantly different as shown in Plate IX which illustrates again the features, shown previously in Plate III.

Selected channels were also extracted from the tooling plates and cold-rolled in a simple, multiple-pass rolling schedule to produce tape/ribbon. Examples of these experiments, which were quite successful from a

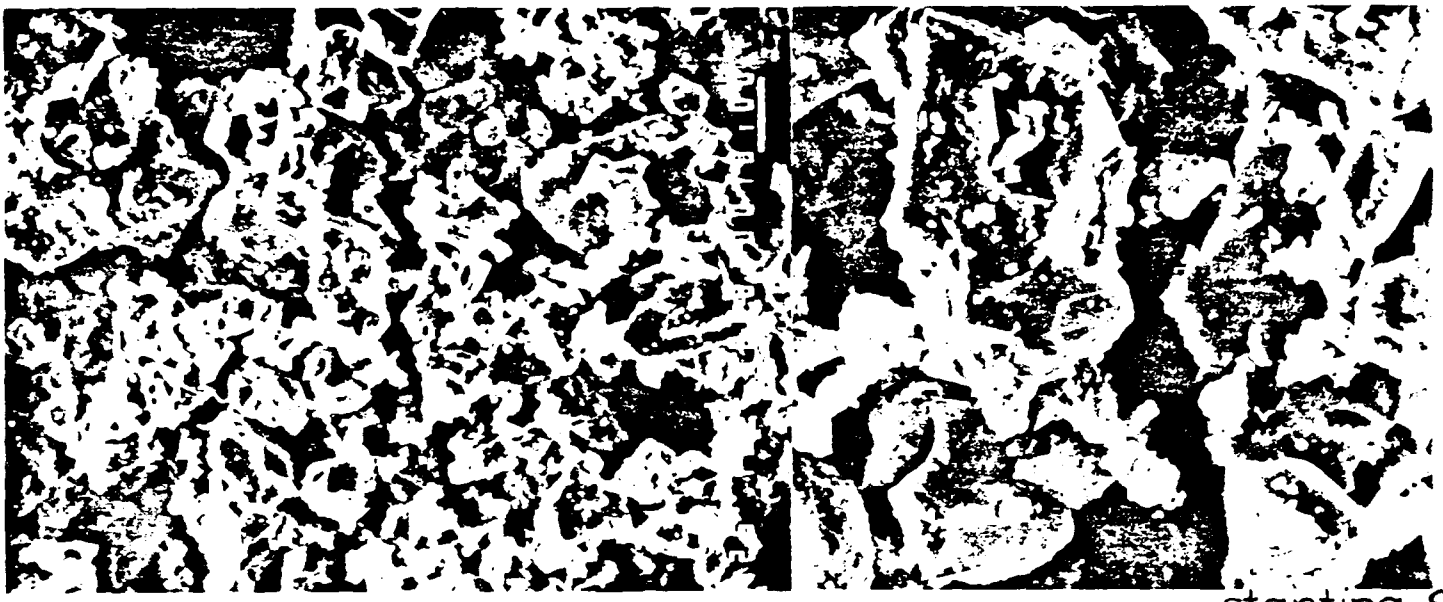

starting S
powder

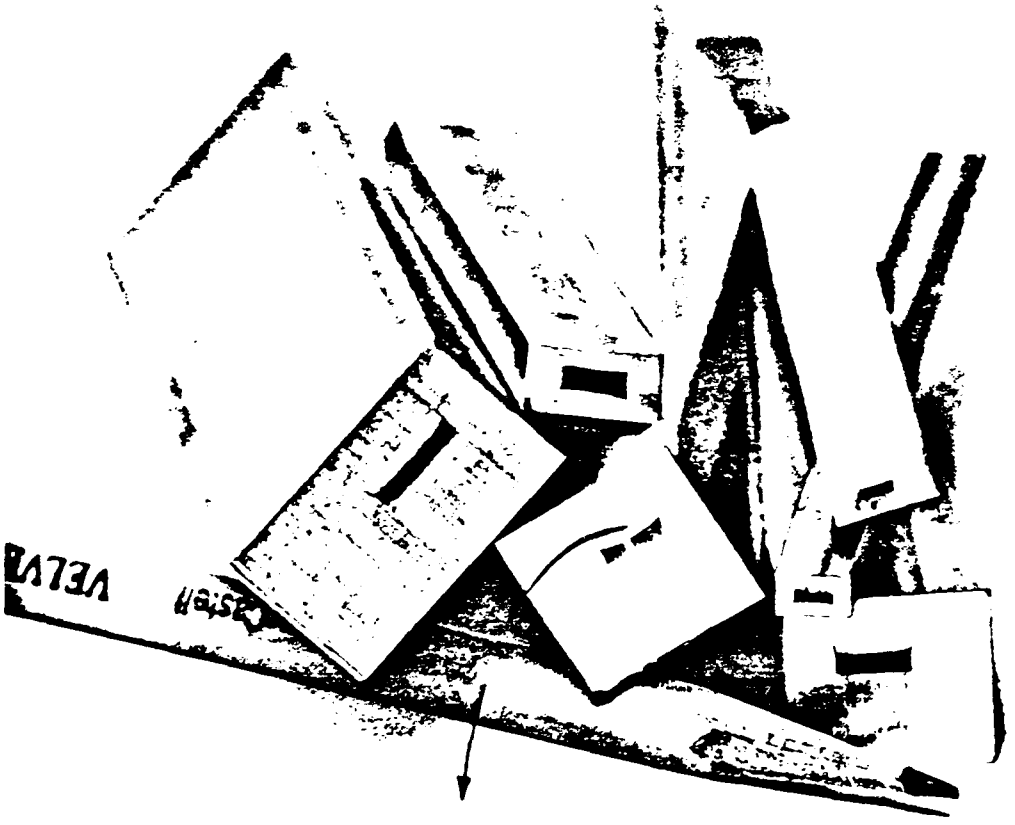

Plate VI

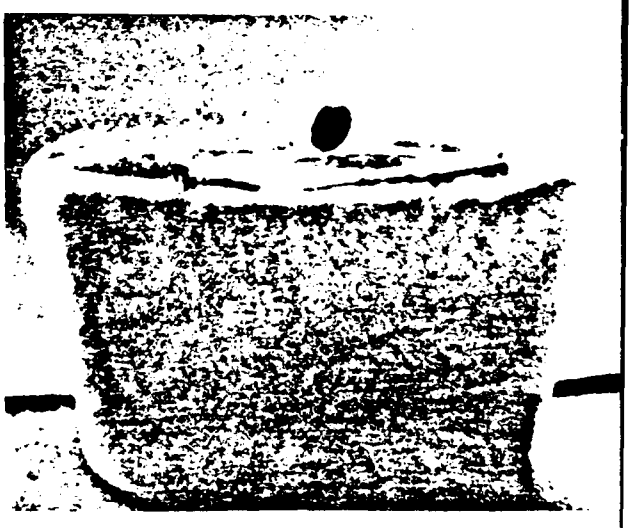

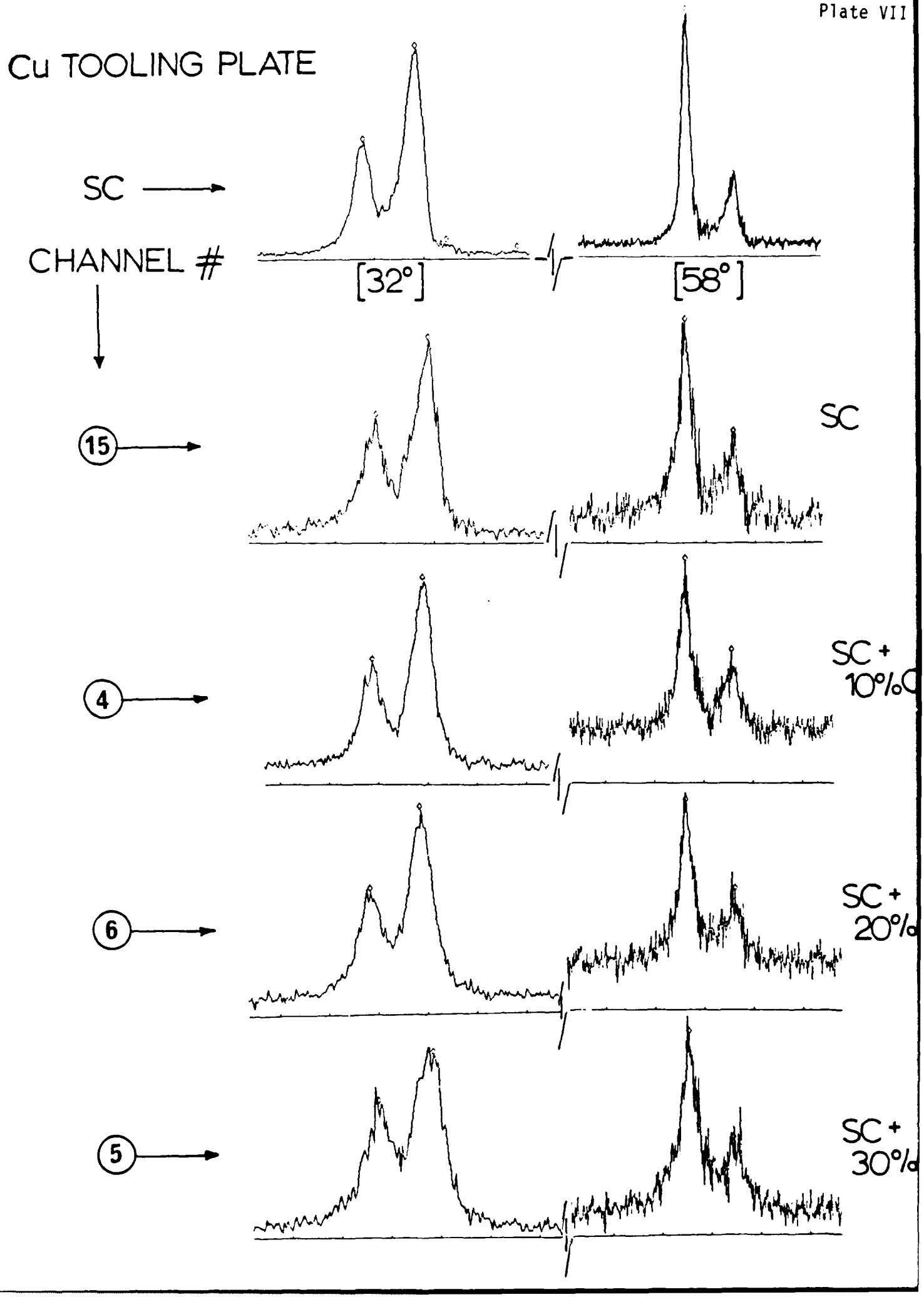
Cu TOOLING PLATE
SC
CHANNEL #
[32°]
[58°]
15
SC
4
SC + 10%C
6
SC + 20%
5
SC + 30%

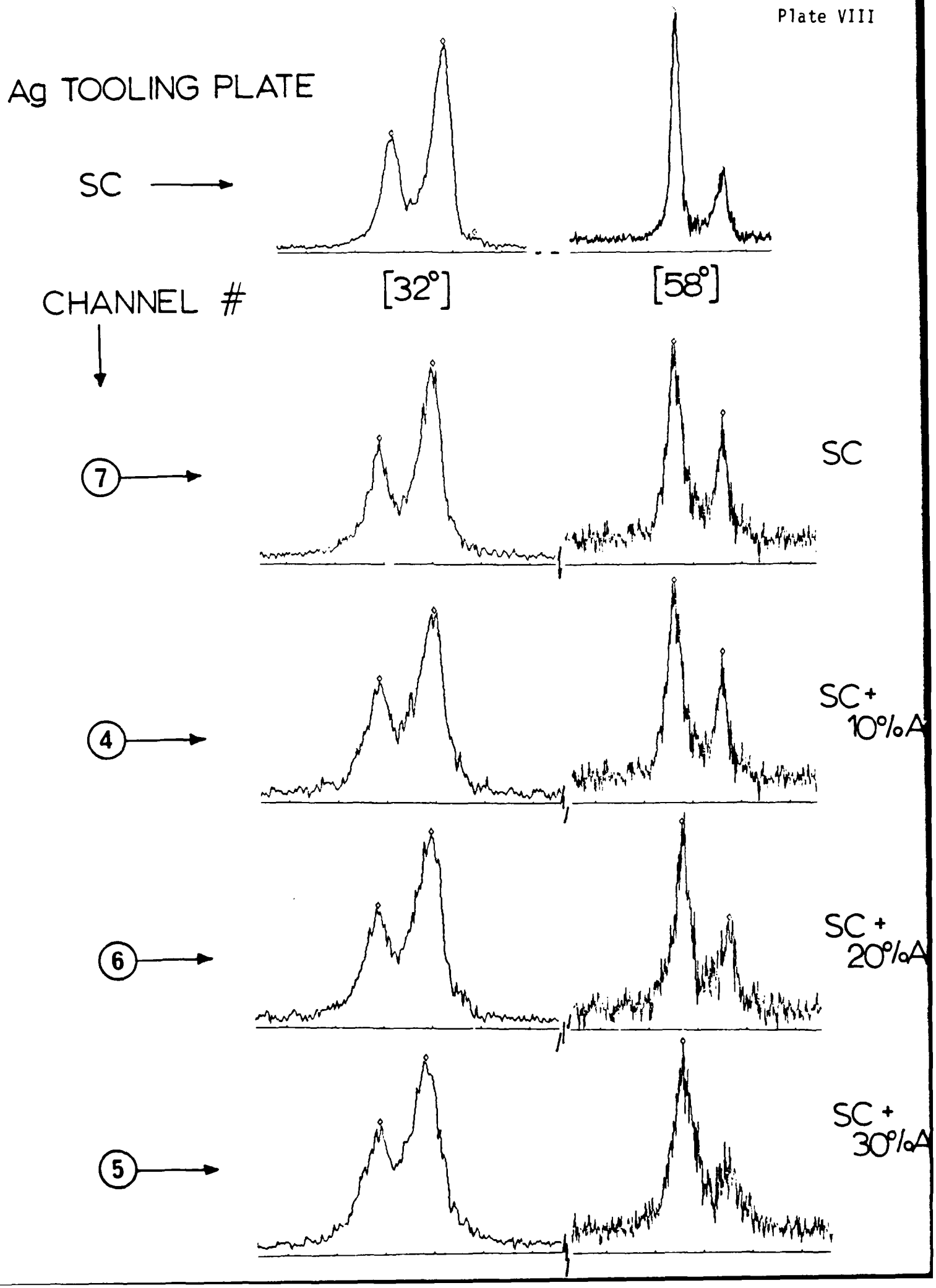
Ag TOOLING PLATE
SC
[32°]
[58°]
CHANNEL #
7
SC
4
SC + 10%A
6
SC + 20%A
5
SC + 30%A

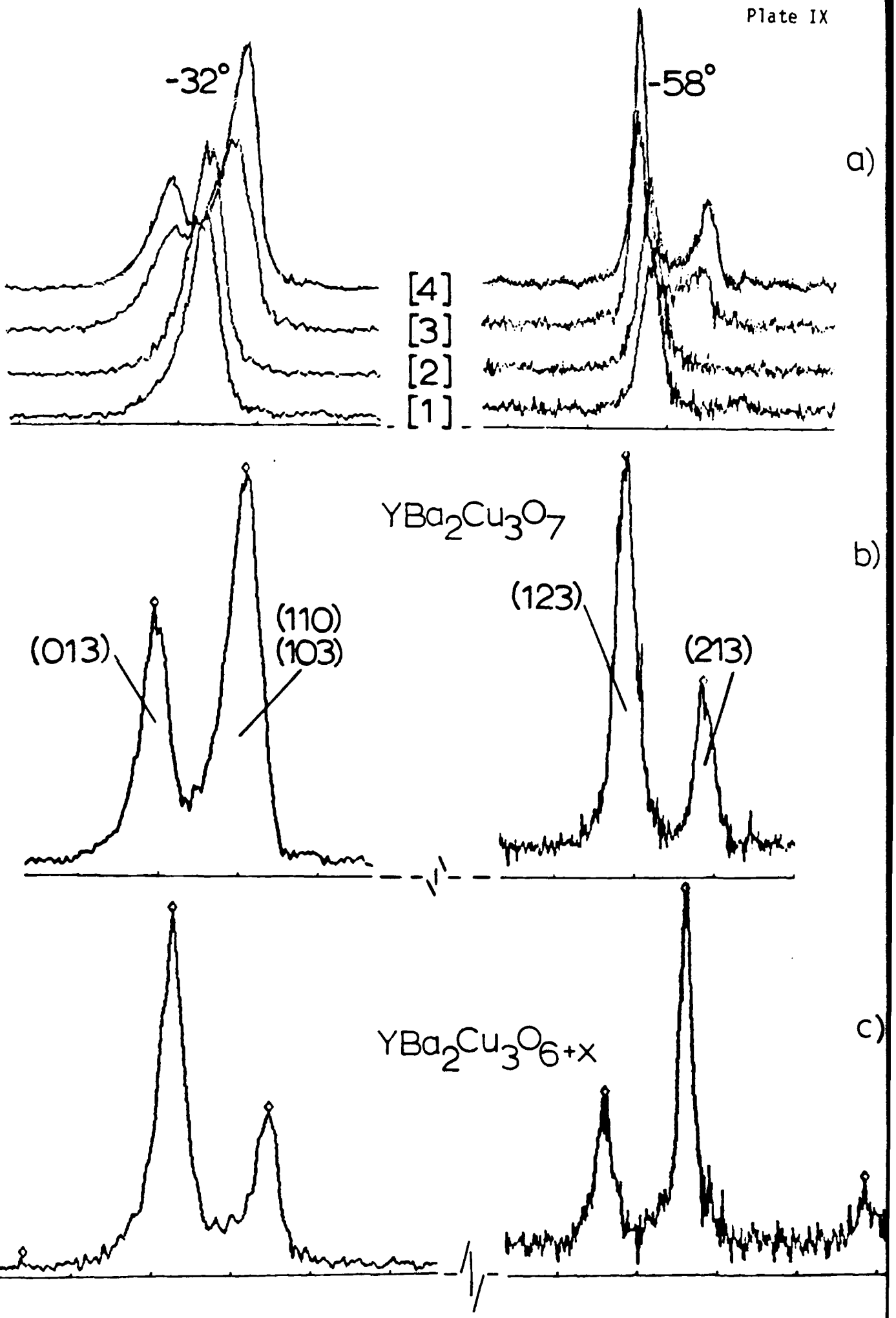
-32°
-58°
a)
[4]
[3]
[2]
[1]
$YBa_2Cu_3O_7$
b)
(013)
(110)
(103)
(123)
(213)
$YBa_2Cu_3O_{6+x}$
c)

process perspective, are shown in Plates X to XII. Plates XI and XII show examples of several passes in the reduction of both the copper and silver precursors. The final ribbon shown in Plate X was approximately 0.005 in. (0.15 mm) thick for both the copper and silver.

While these tapes were not superconducting, both were electrically continuous and exhibited a semiconducting behavior prior to any heat treatment.

In preliminary heat treatment of several channel examples from the Ag tooling plate, we observed some examples of irregular melting within sections of certain channels and gas emission even at low temperatures (400-500°C). We also observed evidence of pressurized gas within Channel #9 in the Ag tooling plate (see Plate V). This evidence coupled with the lack of supercurrent transport behavior and the observable distortion of the initial split-peak x-ray signatures (Plates XI and XII) led us to conclude that in the well-machined tooling plates (Plate V), trapped gas may have created unwanted, local heating within the channels. We, therefore, altered the tooling design for the next experimental series to allow for evacuation prior to and during the explosive fabrication event.

RESULTS AND DISCUSSION OF SERIES 2 TOOLING PLATES (A & B PLATES IN COPPER)

The vacuum tooling plate design utilized in the series 2 explosive fabrication experiments is illustrated in Plates XIII to XV. While the detonation velocity, V_D, was maintained at 2200 m/s, the experimental set up shown in Plate XIV was modified from the first series (Plate V) to develop a better bond between the cladding plate and the tooling (base) plate. The cladding plate thickness was 0.25 in. as well as the stand-off (d_s in Plate XIV). The tooling plates in Plate XIV were essentially

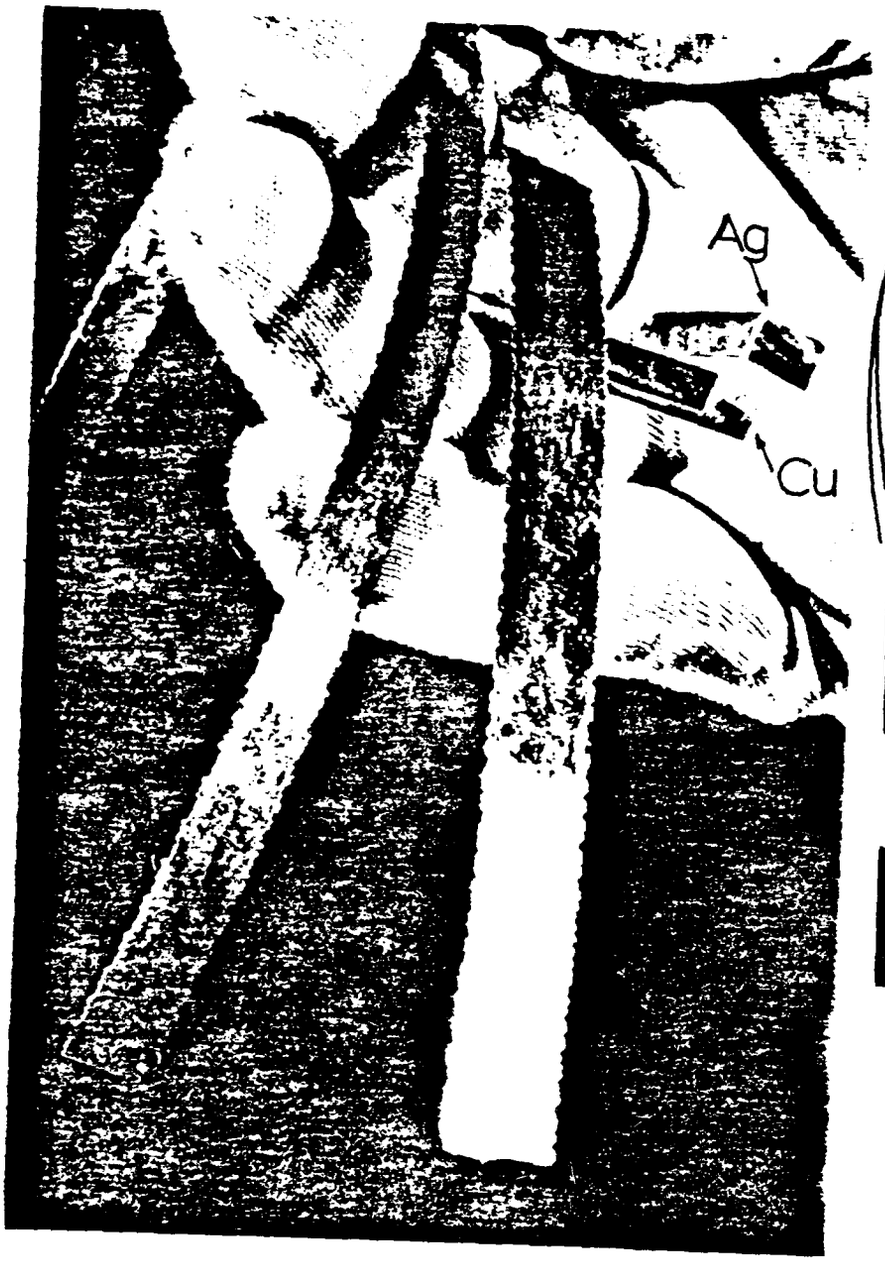

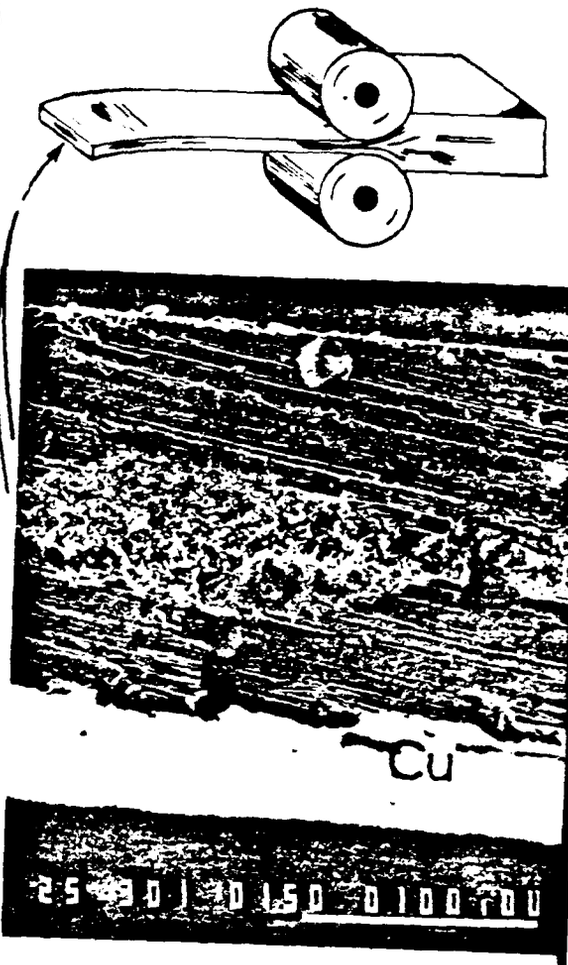

Plate X

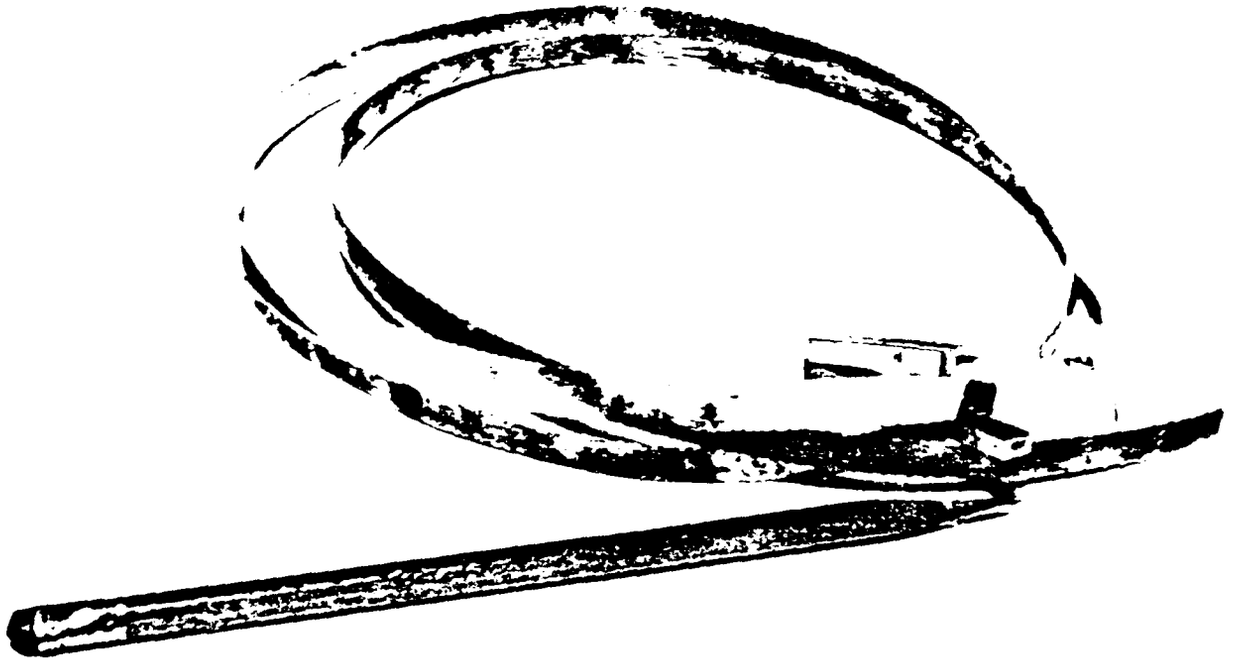

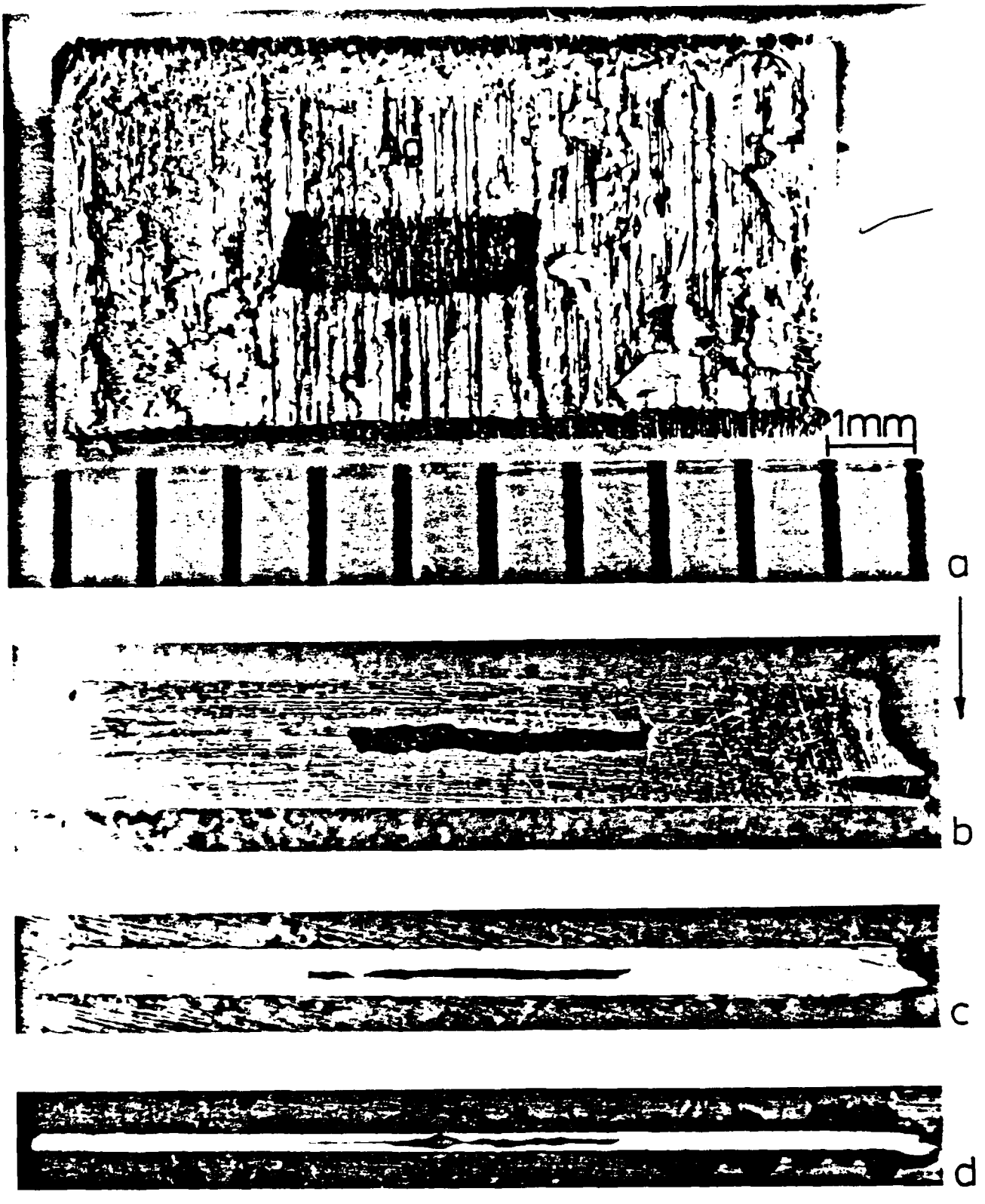

Plate XI

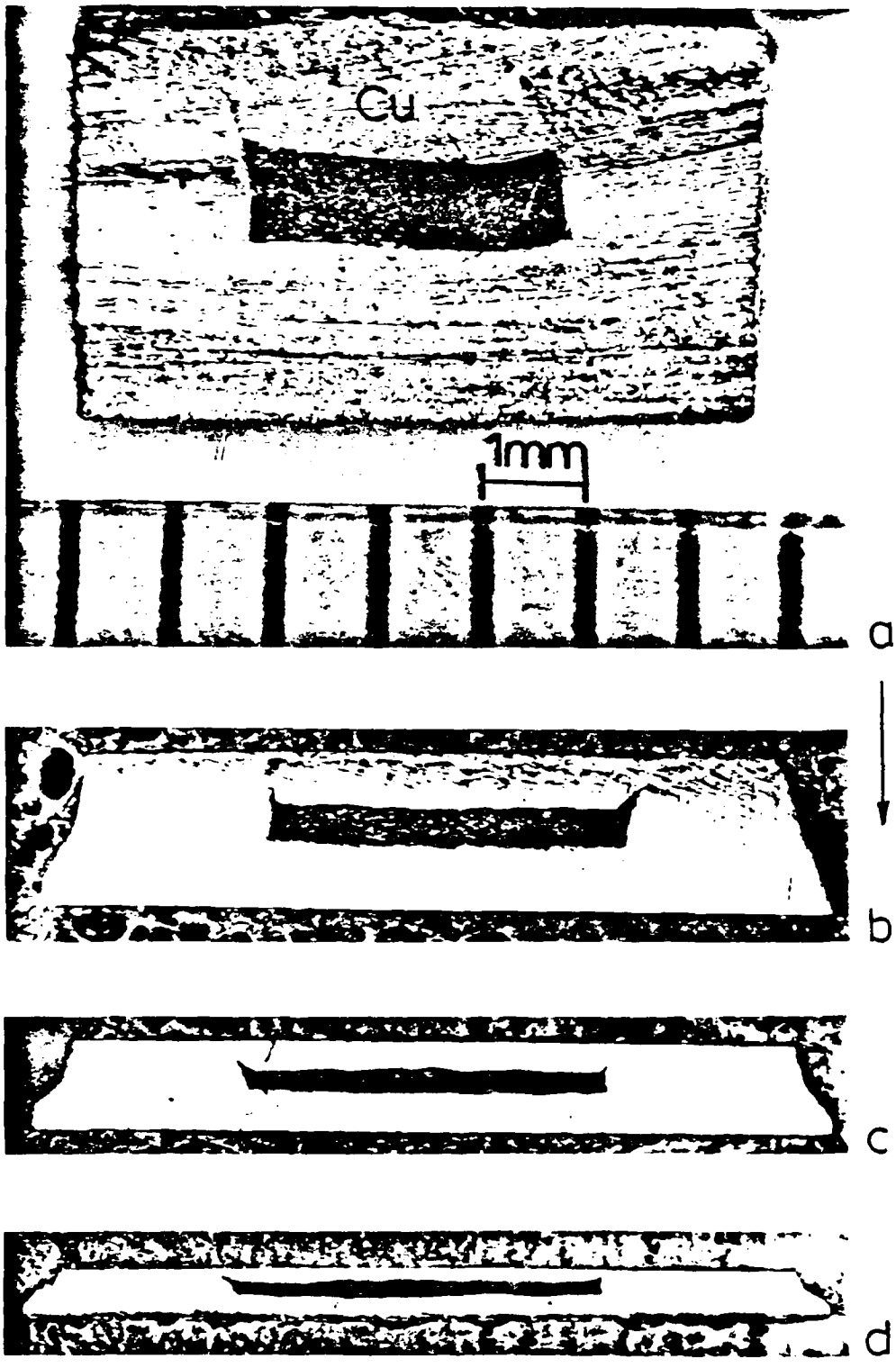

Plate XII

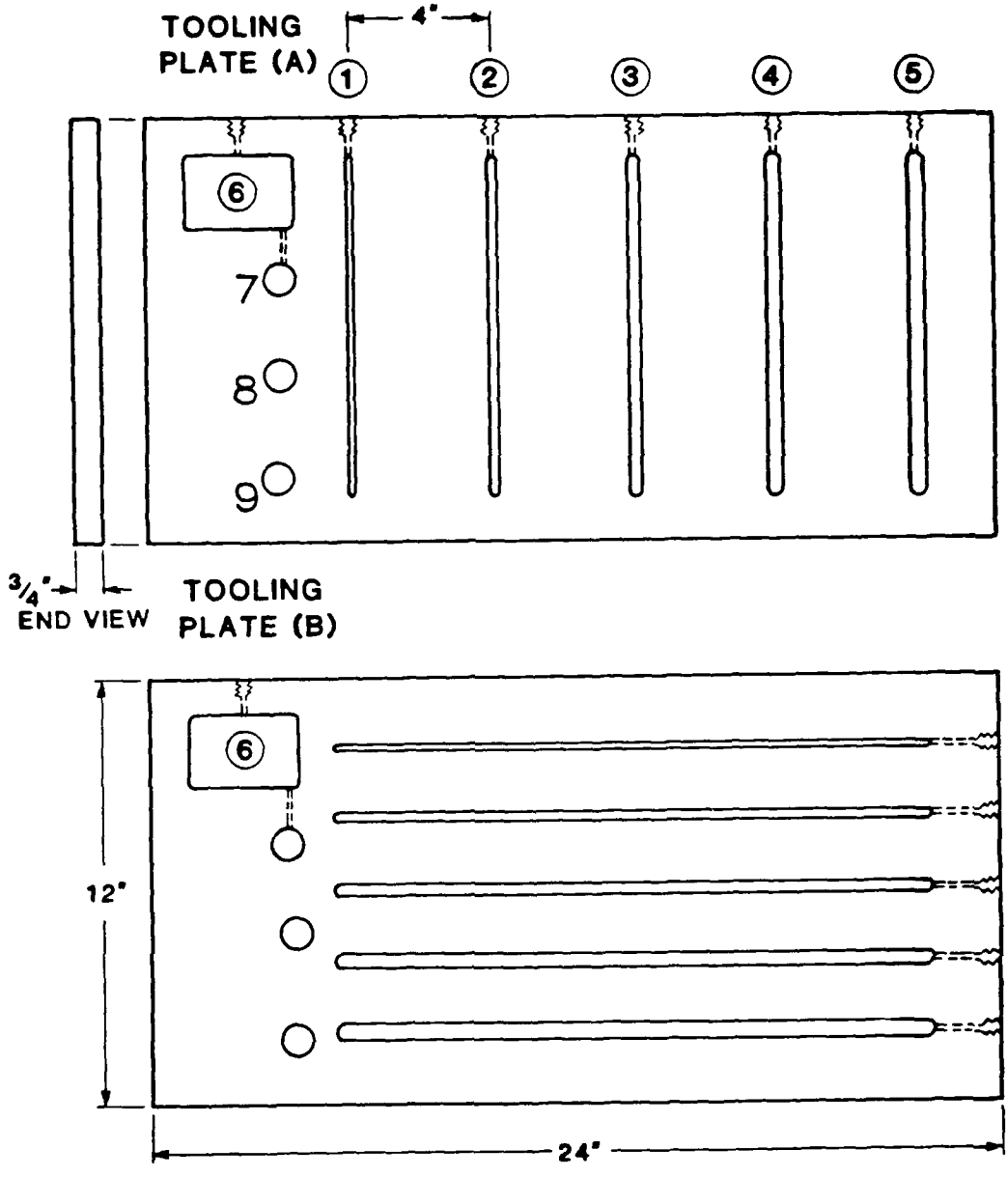
TOOLING
PLATE (A)
4"
1
2
3
4
5
6
7
8
9
3/4"
END VIEW
TOOLING
PLATE (B)
6
1
2
3
4
5
2"
12"
24"

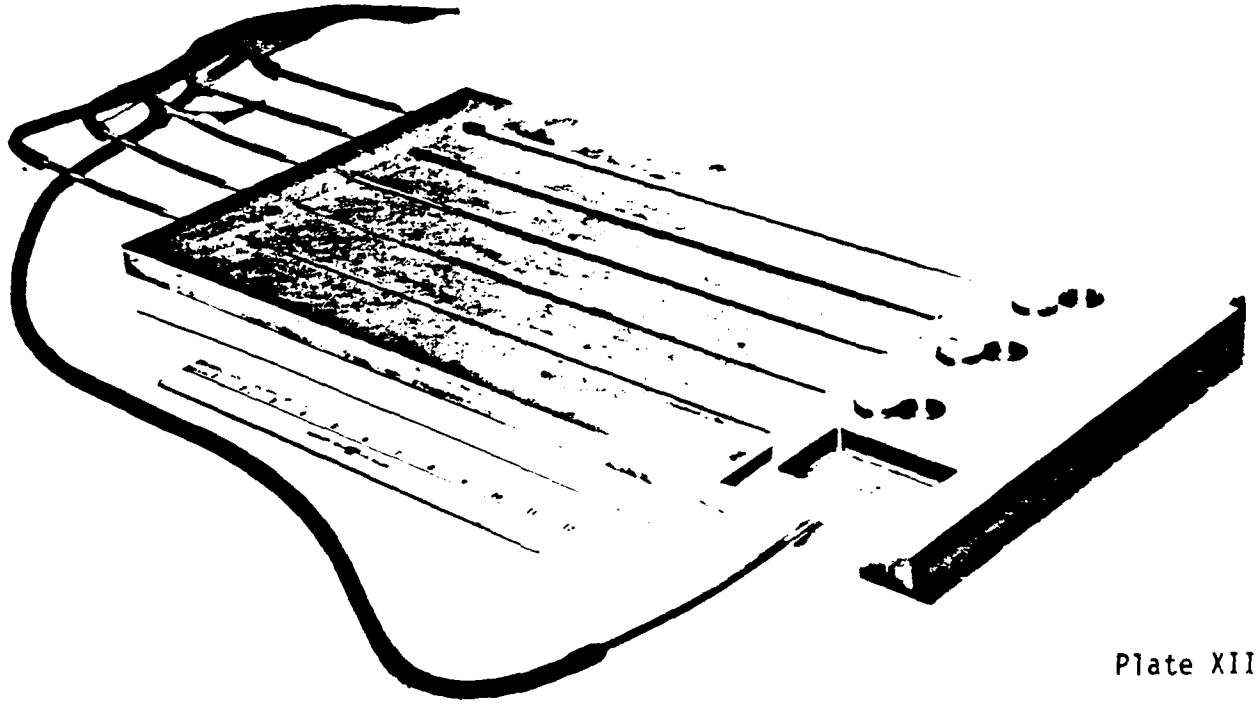

Plate XIII

Plate XIV

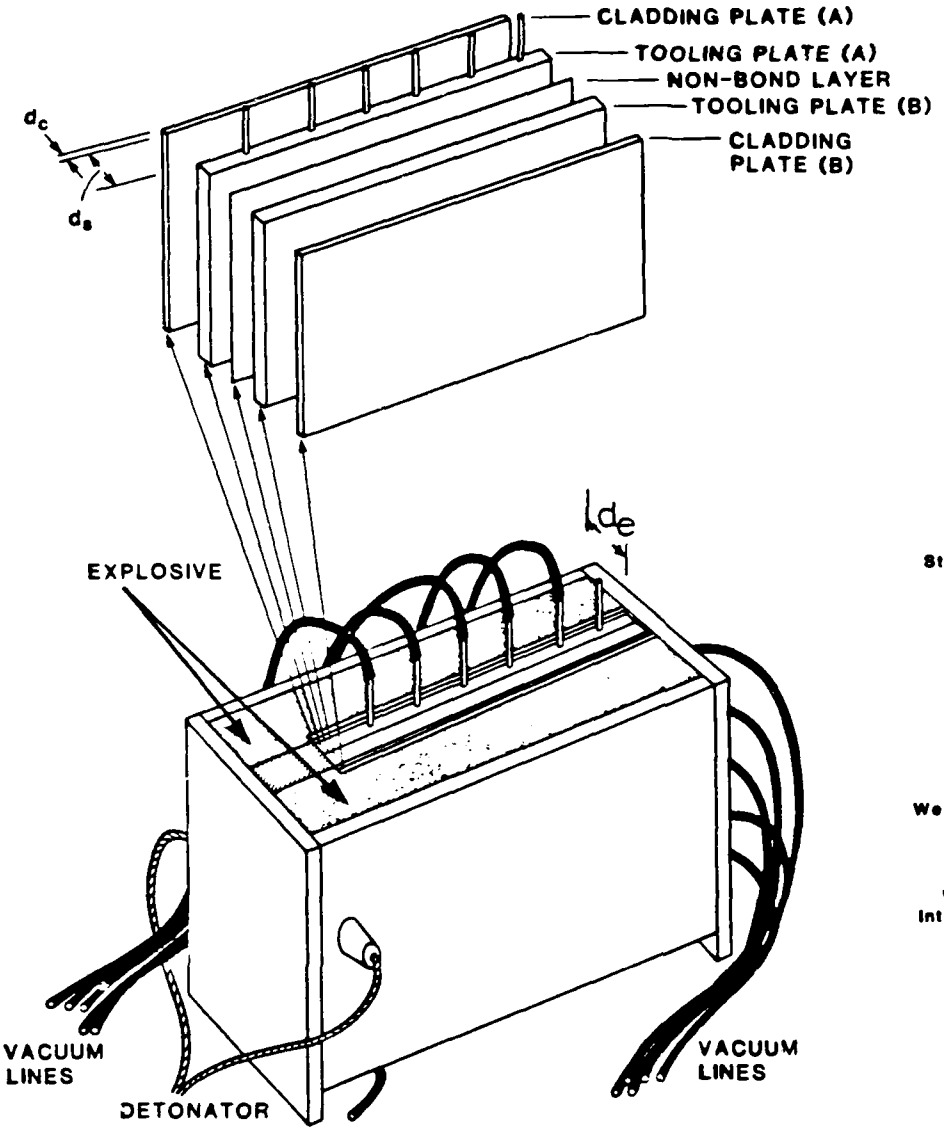

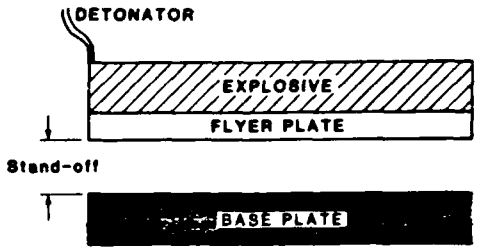

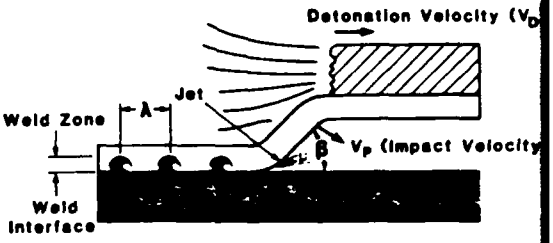

$V_p = 2V_D \sin(\beta/2)$

β = Dynamic Bend Angle
Also Called the Collision Angle

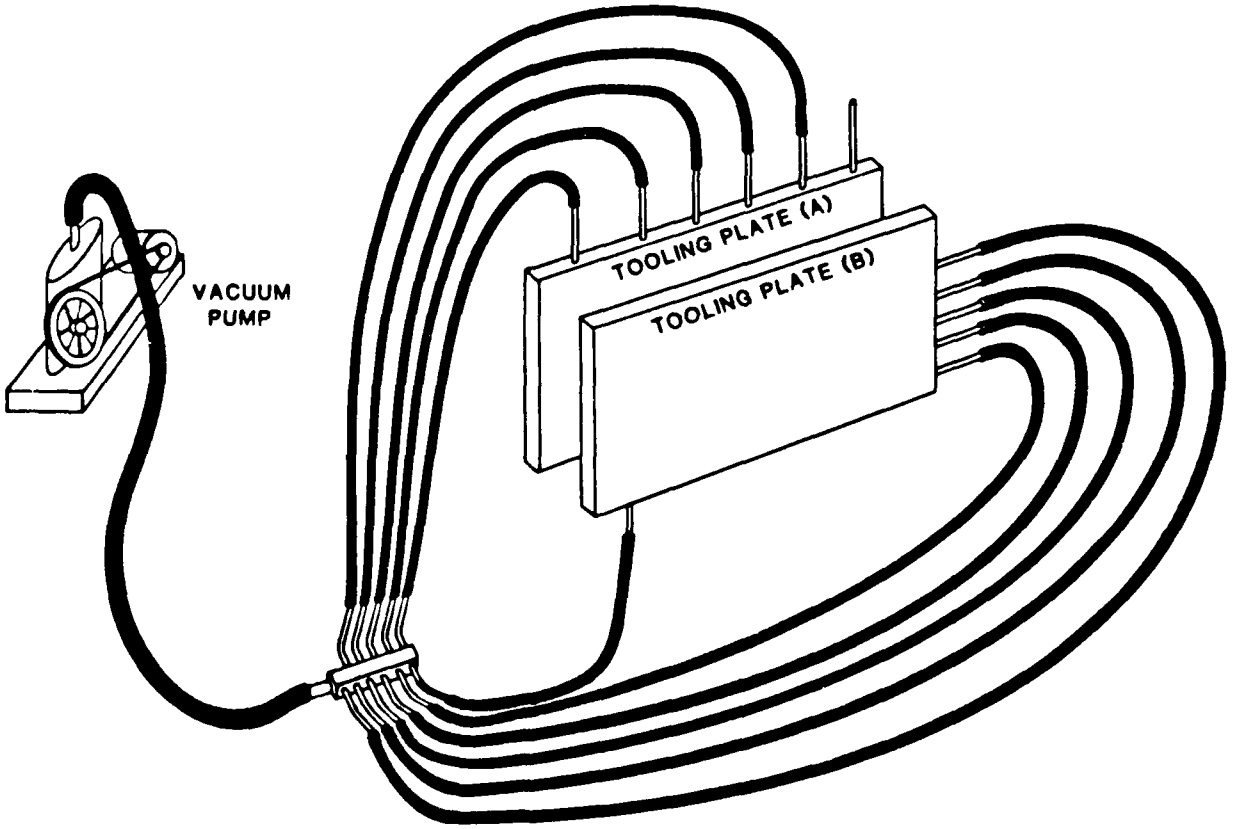

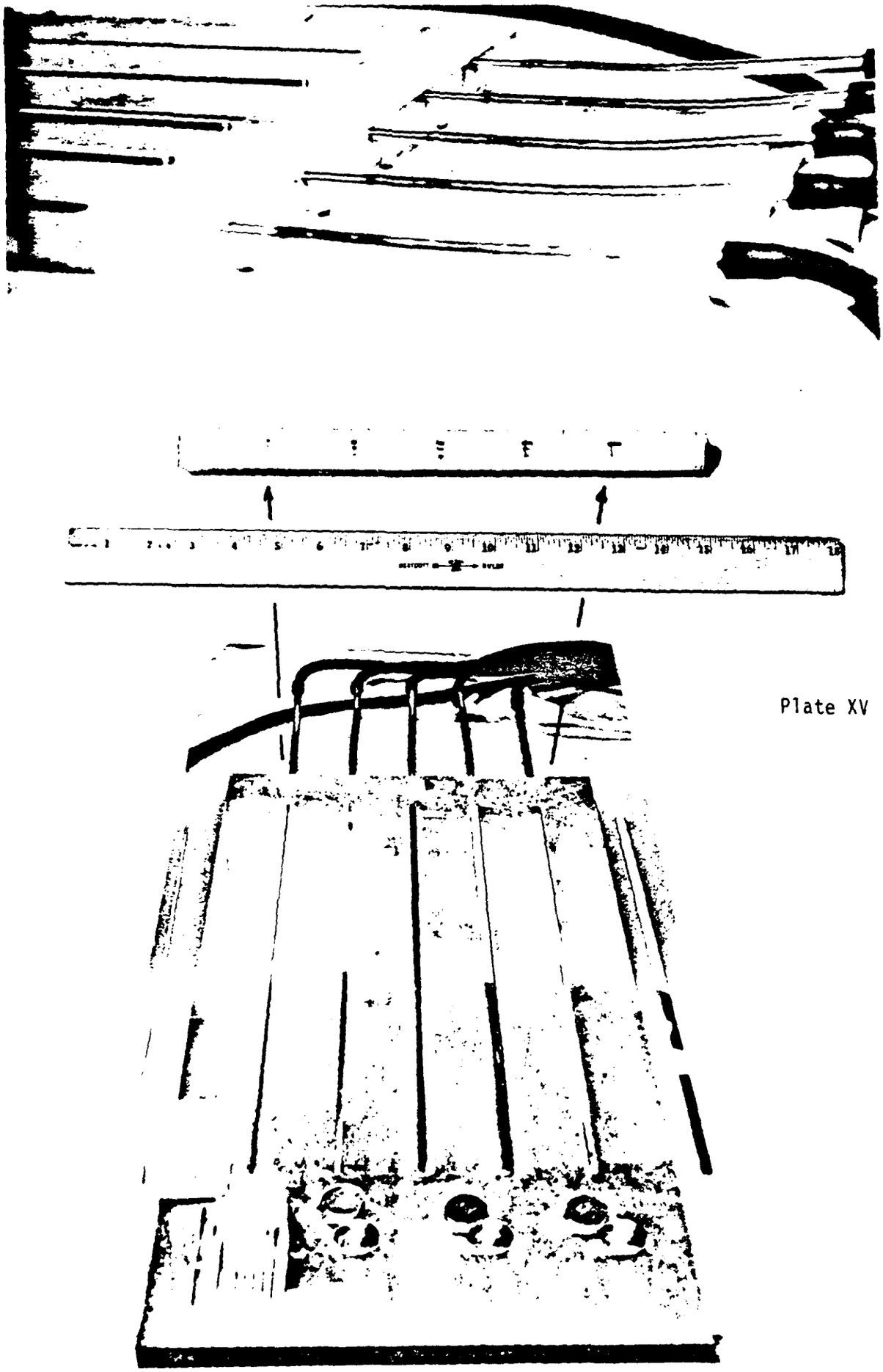

Plate XV

doubled in size from the first Ag/Cu series (Plate V), and the channels were designed to test the effect of orthogonal geometries (parallel and perpendicular to the jet direction) and the possible effect of channel aspect ratio (channel height to width) and scaling of the superconductor cross section. We also placed a large area channel in each tooling plate to begin to examine sandwich features and the ability to scale larger-area fixtures. (Channel #6 in tooling plates A & B--Plate XIV). Channels were also vacuum checked prior to explosive fabrication and the vacuum pump was kept running during the explosive event.

Plate XV illustrates the appearance of the superconducting channel cross sections in tooling plate B after the explosive fabrication by sawing the end off the plate. The channels again exhibited a semiconducting behavior and appeared to be even more poorly developed than the initial Ag/Cu series (Plate V).

X-ray diagnostics of the linear channels as shown in Plates XVI to XVIII clearly reveal more severe superconductor degradation than in the previous fabrication series (Ag/Cu tooling plates).

It was interesting to note that in Tooling Plate A (Plate XVII) channel #5 was not evacuated and the split-peak x-ray signatures seem to be slightly less degraded than the other evacuated channels. Furthermore, evidence of melt spikes below the cover plates and within the superconducting powder channels were observed in tooling plate B, and these spikes appear at first blush to be associated with rather prominent vortex structures which characterized the welding of the cladding plate to the tooling plate and cover plates. This will be further studied in detail.

It is apparent that, in the few steps we have taken, we are heading in the wrong direction--away from the fabrication "window". This simple

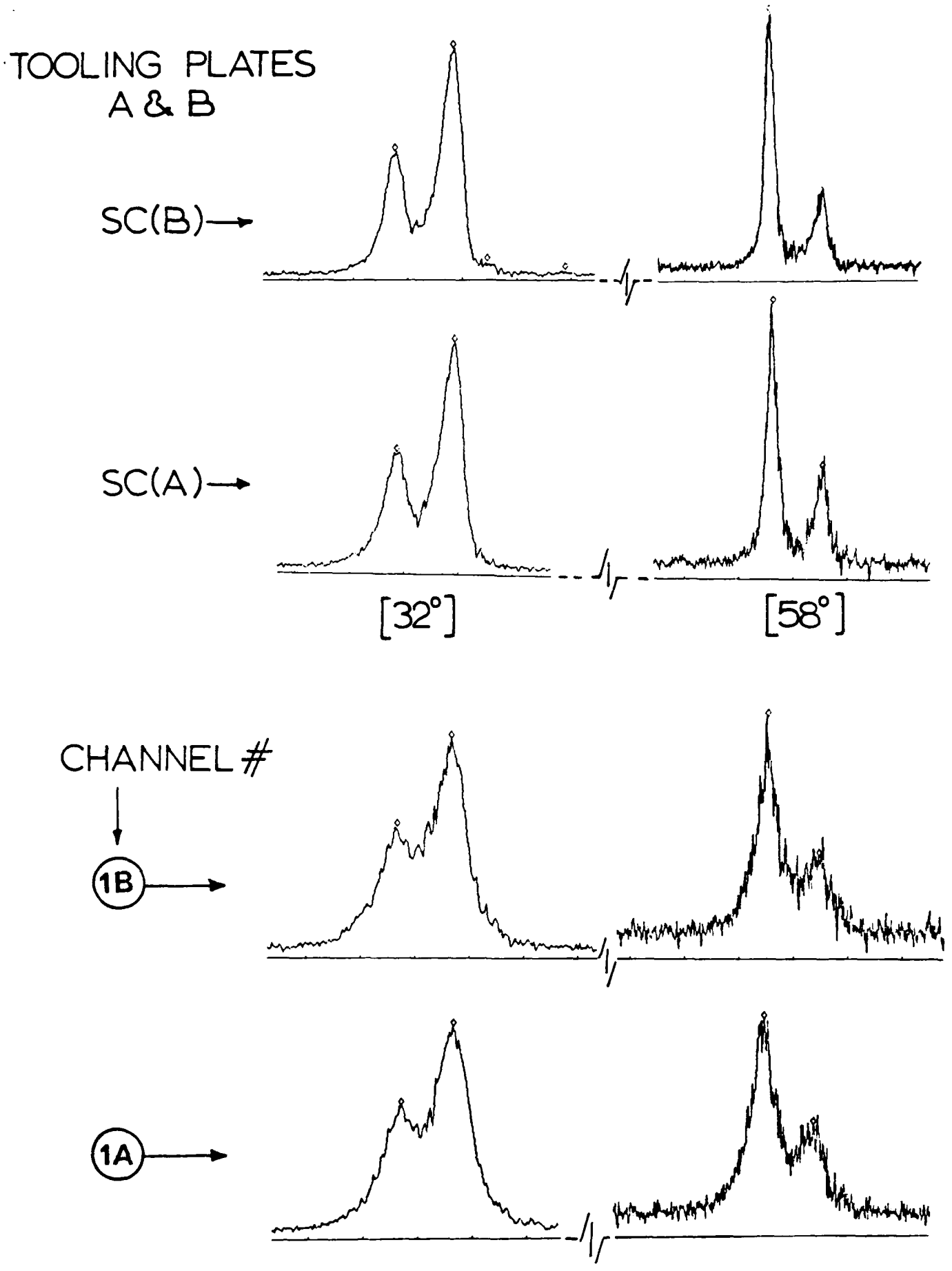

Plate XVI

TOOLING PLATE A

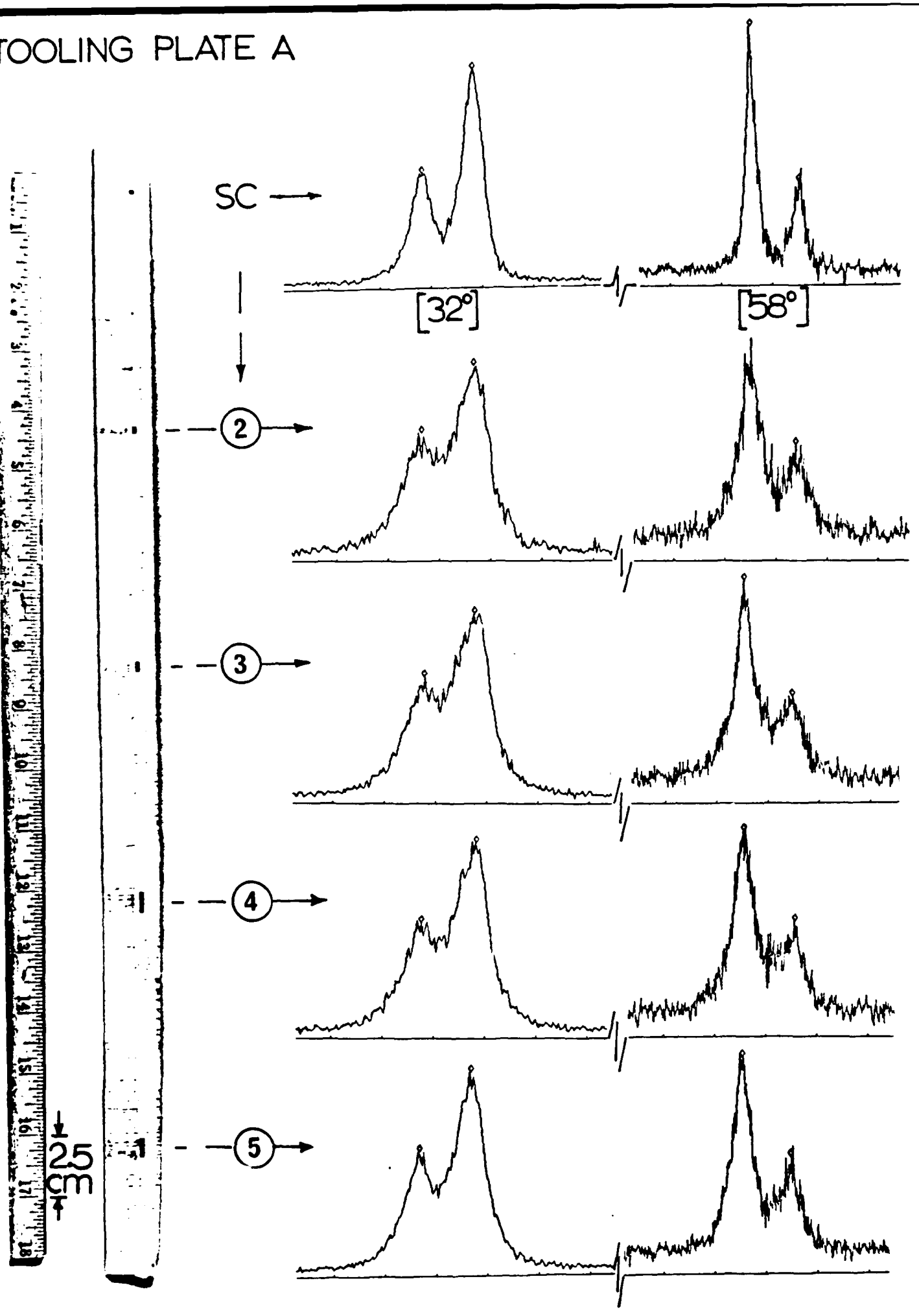

Plate XVII

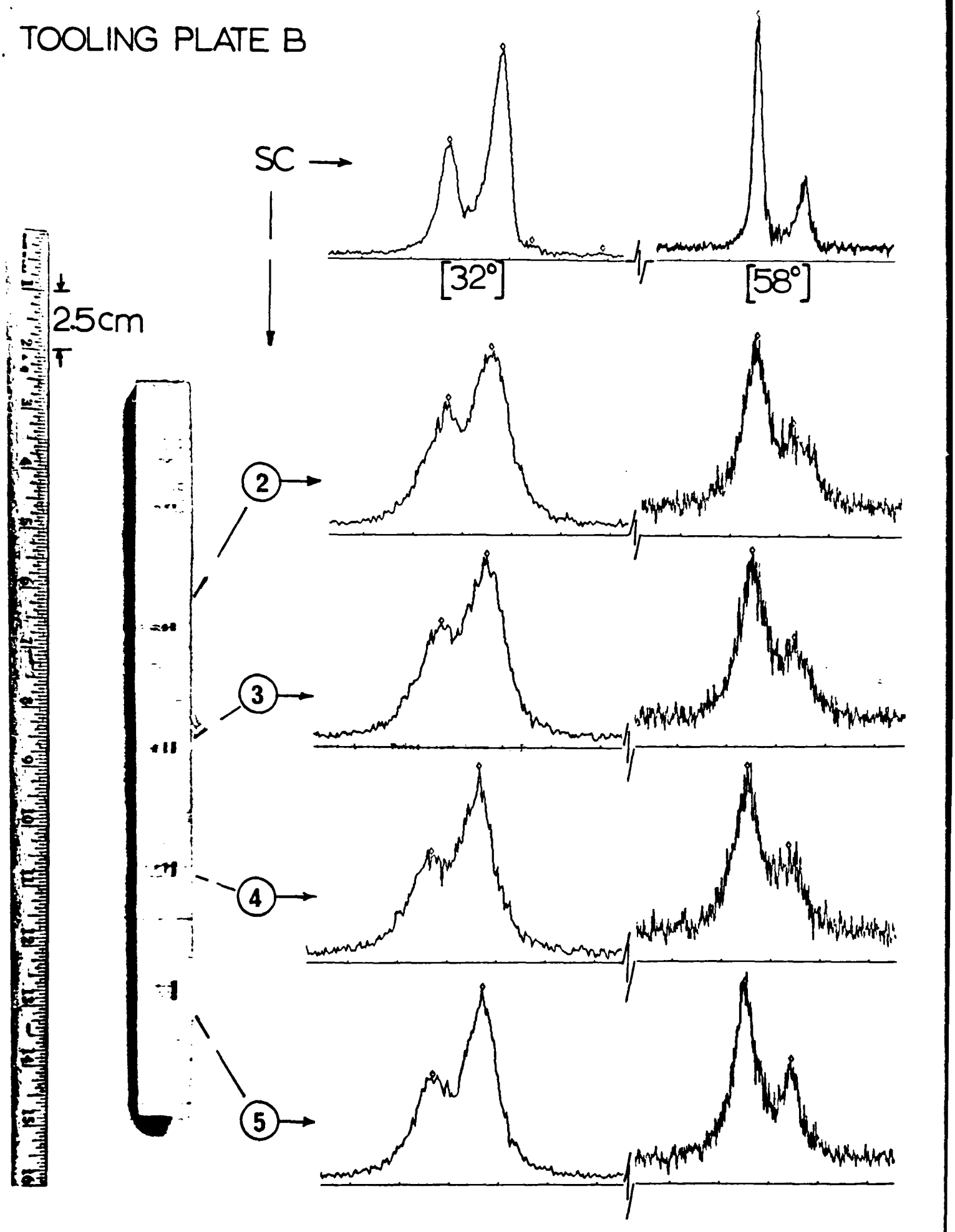

Plate XVIII

series of experiments has demonstrated how complex the interrelationships of fabrication variables seem to be. It also points up the fact that each experiment must be carefully evaluated before a simple series of parameter testing can be conducted. To say this in simple terms--this is a real research program. We don't know the answers nor do we have a clear sense of the questions.

CONCLUSIONS, ANALYSIS, AND RECOMMENDATIONS

While the split-peak x-ray signature diagnosis is not well developed or understood, it has been demonstrated to be a useful, qualitative guide in our search for fabrication guidelines in producing superconducting monoliths. It may be possible, by careful control of superconducting powder and powder size distribution and sample compaction and geometry, to quantify the x-ray peak ratios using a calibrated correlation with magnetic susceptibility measurements. We would not expect the accuracy to be very precise, but quantitation could augment the qualitative difference which is already apparent from our results.

We will also continue our efforts to identify the fundamental reasons for the split-peak x-ray signature changes. It is important to know whether the degradation we have observed is due to oxygen loss or oxygen disorder, and the role that a distribution of non-superconducting phase will play both in the lack of transport supercurrent and in the peak signature changes.

We have demonstrated that very intricate tooling plate designs, including specific channel evacuation, can be achieved, and that considerable scaling of channels and channel dimensions is possible. We have not observed in our most recent experiments significant effects of channel aspect

ratios on the consolidation of superconducting powder within specific channel geometries. However, the consolidation is not optimized, and bulk densities are not better than 90%.

We have demonstrated that very thin ribbon can be very easily cold rolled from explosively fabricated billets, and that, in fact, these precursor geometries containing rectangular superconducting channel cross sections may have some advantage over superconductor-filled and swaged or drawn metal tubes. Moreover, the shock-wave induced microstructures may have a significant effect on the recrystallization and grain growth of the heat-treated tapes or ribbon, but this speculation must be demonstrated experimentally.

We have been able to fabricate a host of channel structures containing metal powder loadings--copper powder mixed with Y-Ba-Cu-O and silver powder mixed with Y-Ba-Cu-O ranging from 10 to 30 volume percent. We have not fully evaluated the many experimental variances afforded by such composite mixtures. One particularly interesting experiment being conducted is the examination of the influence of metal loading on the levitation of a magnet as an indication of the "Meissner fraction" and the influence of metal loading on the volumetric diamagnetism. These experiments may indirectly relate to the determination or calibration of superconducting fraction as indicated in Eqn. (6). On the other hand, the influence of metal loading on mechanical properties and related superconduction phenomena will also be examined.

Metal loading, particularly silver powder additions, even in other metal matrix monoliths, may have important contributions to electrical contact behavior. Electrical contacts are a serious problem in consolidated Y-Ba-Cu-O.

Contact problems are indeed the next level of interfacial problems to consider in this fabrication concept because of the potential problems of consolidated superconducting particle/channel metal contact.

In our earlier assessments of the problems in optimizing the explosive fabrication of superconducting (Y-Ba-Cu-O) metal matrix composite monoliths, we considered the principal considerations to be: 1) the starting Y-Ba-Cu-O quality, especially "clean" surface material; 2) the powder size distribution; and 3) the peak shock pressure. These are the principal considerations in a simple axisymmetric (cylindrical) fabrication process. But, our process is not axisymmetric, and we are now convinced that we must take a more serious look at the specific features of the fabrication geometry, and put the important parameters into some experimental context. We must also look at the prospects of having to optimize a process with numerous, related processing parameters, and this may require experiments performed on an EVOP-Programmed basis--a computer analysis of process variables and an optimization of critical experiments to provide these parameters.

As illustrated in Plate XIV, the explosive fabrication arrangement is a modified explosive welding arrangement where the base plate in the welding process becomes the tooling plate into which the superconducting powder is placed. When the process works efficiently, the metal plates are all welded together, the powder is consolidated, and even bonded to the channel walls, creating a monolithic metal matrix composite. The welding process itself has a number of process variables and the powder consolidation is not a simple axisymmetric case. In order to achieve a superconducting monolith, a number of process variables must be more rigorously identified

and optimized. And because they are interrelated, the optimization is more complex.

References

1. L. E. Murr, A. W. Hare, and N. G. Eror, Nature, 329, 37 (1987).

2. L. E. Murr, A. W. Hare, and N. G. Eror, Adv. Mater. & Processes, 132 (4), 36 (1987).

3. L. E. Murr, T. Monson, J. Javadpour, M. Strasik, U. Sudarsan, N. G. Eror, A. W. Hare, D. G. Brasher, and D. J. Butler, J. Metals, 40 (1), 19 (1988).

4. See K. P. Staudhammer and L. E. Murr in Chap. 7 of Shock Waves for Industrial Applications, L. E. Murr (ed.), Noyes Publications, Park Ridge, NJ, 1988, p. 237.

5. L. E. Murr, T. Monson, M. Strasik, U. Sudarsan, N. G. Eror, and A. W. Hare, J. Superconductivity, 1 (1), 3 (1988).

6. J. R. Clem, Physica C, 153-155, 50 (1988).

7. C. J. Lobb, D. W. Abraham, and M. Tinkham, Phys. Rev. B27, 150 (1983).

8. L. E. Murr and N. G. Eror, Adv. Materials & Manufacturing Processes, December 1988 (in press).